

# Ligand Electronic Effect on Reductive Elimination of Biphenyl from *cis*-[Pt(Ph)<sub>2</sub>(diphosphine)] Complexes Bearing Electron-Poor Diphosphine: Correlation Study between Experimental and Theoretical Results

Toshinobu Korenaga,\* Kayoko Abe, Aram Ko, Ryota Maenishi, and Takashi Sakai\*

Division of Chemistry and Biochemistry, Graduate School of Natural Science and Technology, Okayama University, 3-1-1 Tsushima-naka, Okayama 700-8530, Japan

Received January 28, 2010

The reductive elimination of biphenyl from *cis*-[Pt(Ph)<sub>2</sub>(diphosphine)] (**3**) was studied to clarify the electronic effects of diphosphine ligands on the reaction. Reaction kinetic data were evaluated in *d*<sub>8</sub>-toluene within 80–110 °C using 1,2-bis(diphenylphosphino)ethane (dppe) and seven of its fluoroaromatic analogues as ancillary diphosphine ligands. The fastest reaction rate corresponded to **3**, bearing the electron-poor 1,2-bis[bis(pentafluorophenyl)phosphino]ethane (dfppe) ligand, and was 1240 times faster than that for dppe-bearing **3**, which has the slowest. The estimated rate constants *k* were highly correlated with Taft's  $\sigma^*$  values for phosphorus-bound aromatics in **3**. However, their correlation was split between 2,6-fluorine aromatic and 2,6-hydrogen aromatic-bearing diphosphines, suggesting steric effects from the 2,6-fluorine atoms. The observed  $\Delta H^\ddagger$  values were correlated with theoretical values, which were calculated by the DFT method. The correlations revealed that electron-poor diphosphine ligands decrease the energy gaps between the HOMO–1 of **3** and the HOMO of transition state **3-TS**, including the platinum d orbital, and reduce the destabilization of the platinum d orbital upon binding with the diphosphine in **3-TS** as compared to the cases of an electron-donating ligand. This last mentioned effect is the true nature of electronic influence of the electron-poor diphosphine ligands in the reductive elimination from **3**.

## Introduction

Reductive elimination is an essential step in many transition metal catalyzed reactions.<sup>1</sup> In particular, carbon–carbon<sup>2</sup> and carbon–heteroatom<sup>3</sup> bond-forming cross-coupling reactions undergo reductive elimination in their catalytic cycles, and this step is occasionally rate-determining in catalysis.<sup>4</sup> The rate of reductive elimination greatly depends on the nature of the central metal (e.g., Ni > Pd > Pt) and on the steric and electronic properties of reactive and ancillary ligands.<sup>1b</sup> The influence of

ancillary phosphine ligands on reductive elimination has been widely studied and shown to mostly be steric. In particular, a large bite angle greatly accelerates reductive elimination for bidentate ligands.<sup>1</sup> For example, the rate constant of *cis*-Pd-(CH<sub>2</sub>TMS)(CN)(diphosphine) is accelerated 4760 times by the P–Pd–P bite angle.<sup>5</sup> On the other hand, the electronic effects of ancillary phosphine ligands on the reductive elimination rates have also been reported experimentally.<sup>6</sup> In [Pd(2,5-dichlorophenyl)( $\eta^3$ -2-propenyl){P(C<sub>6</sub>H<sub>4</sub>-R)<sub>3</sub>}], for example, the weakest  $\sigma$ -donor phosphine (R = Cl) led to a reductive elimination that was 5.6 times faster than for the strongest  $\sigma$ -donor phosphine (R = OMe).<sup>6a</sup> Hartwig et al. reported similar accelerations, which were influenced by electronic effects of the ancillary diphosphine ligand in R-1,1'-bis(diphenylphosphino)ferrocene (R-dppf)-ligated palladium complexes.<sup>1c,7</sup> The [Pd(CF<sub>3</sub>-dppf)(C<sub>6</sub>H<sub>4</sub>-4-CN)(OC<sub>6</sub>H<sub>4</sub>-4-OMe)] complex underwent reductive elimination 2 times faster than its analogous dppf complex.<sup>7c</sup> Similarly, reductive elimination was 6.5 times faster for [Pd(CF<sub>3</sub>-dppf)(C<sub>6</sub>H<sub>4</sub>-4-CF<sub>3</sub>){N(Me)-*p*-tolyl}] than for the MeO-dppf-ligated analogue.<sup>7d</sup> Although less  $\sigma$ -donating phosphines accelerated the reductive elimination in those results, electronic effects were not as significant as bite

\*To whom correspondence should be addressed. E-mail: korenaga@cc.okayama-u.ac.jp.

(1) Reviews: (a) Brown, J. M.; Cooley, N. A. *Chem. Rev.* **1988**, *88*, 1031. (b) Ozawa, F. In *Fundamentals of Molecular Catalysis*; Kurosawa, H., Yamamoto, A., Eds.; Elsevier: New York, 2003; Vol. 3, p 479. (c) Hartwig, J. F. *Inorg. Chem.* **2007**, *46*, 1936.

(2) Recent reviews: (a) Chen, X.; Engle, K. M.; Wang, D.-H.; Yu J.-Q. *Angew. Chem., Int. Ed.* **2009**, *48*, 5094. (b) Phapale, V. B.; Cardenas, D. *J. Chem. Soc. Rev.* **2009**, *38*, 1598. (c) Terao, J.; Kambe, N. *Acc. Chem. Res.* **2008**, *41*, 1545. (d) Martin, R.; Buchwald, S. L. *Acc. Chem. Res.* **2008**, *41*, 1461.

(3) Reviews: (a) Surry, D. S.; Buchwald, S. L. *Angew. Chem., Int. Ed.* **2008**, *47*, 6338. (b) Hartwig, J. F. *Acc. Chem. Res.* **2008**, *41*, 1534. (c) Janey, J. M. *Name Reactions for Functional Group Transformations*; Wiley: New York, 2007; p 564. (d) Buchwald, S. L.; Mauger, C.; Mignani, G.; Scholz, U. *Adv. Synth. Catal.* **2006**, *348*, 23. (e) Hartwig, J. F. *Comprehensive Coordination Chemistry II*; Elsevier: Amsterdam, 2004; Vol. 9, p 369. (f) Stuermer, R. *Organic Synthesis Highlights V*; Wiley-VCH: Weinheim, 2003; p 22. (g) Muci, A. R.; Buchwald, S. L. *Top. Curr. Chem.* **2002**, *219*, 131. (h) Hartwig, J. F. *Angew. Chem., Int. Ed.* **1998**, *37*, 2046.

(4) Recent examples: (a) Lanni, E. L.; McNeil, A. J. *J. Am. Chem. Soc.* **2009**, *131*, 16573. (b) Jin, L.; Zhang, H.; Li, P.; Sowa, J. R.; Lei, A. *J. Am. Chem. Soc.* **2009**, *131*, 9892. (c) Boren, B. C.; Narayan, S.; Rasmussen, L. K.; Zhang, L.; Zhao, H.; Lin, Z.; Jia, G.; Fokin, V. V. *J. Am. Chem. Soc.* **2008**, *130*, 8923.

(5) Marccone, J. E.; Moloy, K. G. *J. Am. Chem. Soc.* **1998**, *120*, 8527.

(6) (a) Kurosawa, H.; Emoto, M. *Chem. Lett.* **1985**, 1161. (b) Komiya, S.; Shibue, A. *Organometallics* **1985**, *4*, 684. (c) Negishi, E.; Takahashi, T.; Akiyoshi, K. *J. Organomet. Chem.* **1987**, *334*, 181.

(7) (a) Shekhar, S.; Hartwig, J. F. *J. Am. Chem. Soc.* **2004**, *126*, 13016. (b) Culkun, D. A.; Hartwig, J. F. *Organometallics* **2004**, *23*, 3398. (c) Yamashita, M.; Hartwig, J. F. *J. Am. Chem. Soc.* **2004**, *126*, 5344. (d) Yamashita, M.; Vicario, J. V. C.; Hartwig, J. F. *J. Am. Chem. Soc.* **2003**, *125*, 16347. (e) Mann, G.; Shelby, Q.; Roy, A. H.; Hartwig, J. F. *Organometallics* **2003**, *22*, 2775.

angle effects. This may be due to the small difference in electronic properties between the compared phosphines. Therefore, a more electron-poor ancillary phosphine ligand would result in a greater acceleration of the reaction rate. Although a highly electron-poor phosphine slows down metal coordination in some cases,<sup>8</sup> the use of a bidentate electron-poor diphosphine analogue reduces the lability of the metal complex.<sup>9</sup> Roddick et al. reported the reductive elimination of biaryl from [Pt(Ar)<sub>2</sub>(dfppe)] (dfppe: 1,2-bis[bis(pentafluorophenyl)phosphino]ethane).<sup>10</sup> Their report was summarized as follows. (a) Reductive elimination from [Pt(Ph)<sub>2</sub>(dfppe)] proceeds through a direct path to give biphenyl and [Pt(dfppe)<sub>2</sub>]. (b) Intermolecular exchange does not occur between reactive phenyl groups. (c) An approximately 10-fold elimination rate enhancement was observed in nonpolar solvents such as benzene over polar solvents such as DMSO. (d) The elimination rates from [Pt(Ar)<sub>2</sub>(dfppe)] are of advantage to electron-rich reactive aryl groups. This report showed significant results but does not compare the elimination rates of the dfppe-containing complexes with complexes bearing a more  $\sigma$ -donating diphosphine such as dppe. Therefore, we conducted a kinetic study on reductive elimination from [Pt(Ph)<sub>2</sub>(diphosphine)] complexes formed with several dppe analogues, including fluoroaromatic diphosphines, to compare their reaction rates and evaluate the diphosphine electronic effects. Studies using electronically tuned ligand analogues promise a better understanding of the electronic nature of ancillary diphosphine ligands in reductive elimination. In general, the electronic influence of phosphine ligands has been proposed to contribute to the decrease in electron density at the metal center, thus accelerating reductive elimination.<sup>1</sup> In response, the electronic effects of phosphine ligands have been analyzed using MO or DFT calculations.<sup>11</sup> Although previous reports have described many significant findings regarding the electronic effects of some phosphines, their major focus was to clarify whether the mechanism of reductive elimination followed a direct or a dissociative path<sup>1</sup> using monodentate phosphines. Therefore, the electronic effects of ancillary phosphine ligands in reductive elimination may not have been clarified sufficiently. Hence, we also performed DFT calculations for our system and correlated the computational results with experimental values to understand the electronic effects of diphosphines in reductive elimination.

## Results and Discussion

### Preparation and Electronic Property of Diphosphine Ligand 1.

Except for commercially available dppe (**1a**) and dfppe (**1h**),

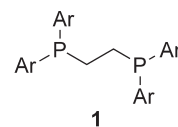
(8) (a) Tiburcio, J.; Bernes, S.; Torrens, H. *Polyhedron* **2006**, *25*, 1549. (b) Clarke, M. L.; Ellis, D.; Mason, K. L.; Orpen, A. G.; Pringle, P. G.; Wingard, R. L.; Zaher, D. A.; Baker, R. T. *Dalton Trans.* **2005**, 1294.

(9) Pollock, C. L.; Saunders, G. C.; Smyth, E. C. M. S.; Sorokin, V. I. *J. Fluorine Chem.* **2008**, *129*, 142.

(10) Merwin, R. K.; Schnabel, R. C.; Koola, J. D.; Roddick, D. M. *Organometallics* **1992**, *11*, 2972.

(11) (a) Tatsumi, K.; Hoffmann, R.; Yamamoto, A.; Stille, J. K. *Bull. Chem. Soc. Jpn.* **1981**, *54*, 1857. (b) Ananikov, V. P.; Musaev, D. G.; Morokuma, K. *Eur. J. Inorg. Chem.* **2007**, 5390. (c) Ariafard, A.; Yates, B. F. *J. Organomet. Chem.* **2009**, *694*, 2075. (d) Ananikov, V. P.; Musaev, D. G.; Morokuma, K. *J. Am. Chem. Soc.* **2002**, *124*, 2839. (e) Hofmann, P. *Organosilicon Chem.* **1994**, 231.

(12) Synthesis of dppe analogues bearing fluoroaryls: (a) Mirabelli, C. K.; Hill, D. T.; Faucette, L. F.; McCabe, F. L.; Girard, G. R.; Bryan, D. B.; Sutton, B. M.; Barus, J. O. L.; Croke, S. T.; Johnson, R. K. *J. Med. Chem.* **1987**, *30*, 2181. (b) Corcoran, C.; Fawcett, J.; Friedrichs, S.; Holloway, J. H.; Hope, E. G.; Russell, D. R.; Saunders, G. C.; Stuart, A. M. *J. Chem. Soc., Dalton Trans.* **2000**, 161. (c) Fischer, R.; Langer, J.; Malassa, A.; Walther, D.; Goerls, H.; Vaughan, G. *Chem. Commun.* **2006**, 2510.



Ar =

- a:** C<sub>6</sub>H<sub>5</sub> (DPPE)    **b:** 4-F-C<sub>6</sub>H<sub>4</sub>    **c:** 3,5-F<sub>2</sub>-C<sub>6</sub>H<sub>3</sub>  
**d:** 2,6-F<sub>2</sub>-C<sub>6</sub>H<sub>3</sub>    **e:** 3,4,5-F<sub>3</sub>-C<sub>6</sub>H<sub>2</sub>    **f:** 2,4,6-F<sub>3</sub>-C<sub>6</sub>H<sub>2</sub>  
**g:** 2,3,5,6-F<sub>4</sub>-C<sub>6</sub>H    **h:** C<sub>6</sub>F<sub>5</sub> (DFPPE)    **i:** 4-CF<sub>3</sub>-C<sub>6</sub>F<sub>4</sub>

**Figure 1.** Diphosphine-bearing fluoroaromatics.

**Table 1.**  $\nu_{\text{C=O}}$  Values of Complex **2**

Ar of diphosphine <b>1</b>	$\nu_{\text{C=O}}$ of <b>2</b> (cm <sup>-1</sup> ) <sup>a</sup>	Taft's $\sigma^*$ of Ar
Et	2012 <sup>b</sup>	-0.10
Ph ( <b>1a</b> )	2021.4 [ <b>2a</b> ]	0.60
4-F-C <sub>6</sub> H <sub>4</sub> ( <b>1b</b> )	2023.4 [ <b>2b</b> ]	0.63
3,5-F <sub>2</sub> -C <sub>6</sub> H <sub>3</sub> ( <b>1c</b> )	2029.6 [ <b>2c</b> ]	1.01
2,6-F <sub>2</sub> -C <sub>6</sub> H <sub>3</sub> ( <b>1d</b> )	2030.1 [ <b>2d</b> ]	1.02
3,4,5-F <sub>3</sub> -C <sub>6</sub> H <sub>2</sub> ( <b>1e</b> )	2031.3 [ <b>2e</b> ]	1.04
2,4,6-F <sub>3</sub> -C <sub>6</sub> H <sub>2</sub> ( <b>1f</b> )	2032.1 [ <b>2f</b> ]	1.08
2,3,5,6-F <sub>4</sub> -C <sub>6</sub> H ( <b>1g</b> )	2038.8 [ <b>2g</b> ]	1.36
C <sub>6</sub> F <sub>5</sub> ( <b>1h</b> )	2040.7 [ <b>2h</b> ]	1.50
4-CF <sub>3</sub> -C <sub>6</sub> F <sub>4</sub> ( <b>1i</b> )	2044.8 [ <b>2i</b> ]	1.75
C <sub>2</sub> F <sub>5</sub>	2064 <sup>b</sup>	2.83
F	2074 <sup>b</sup>	3.19

<sup>a</sup>The highest A<sub>1</sub> stretching mode in CH<sub>2</sub>Cl<sub>2</sub>. <sup>b</sup>From ref 15.

diphosphines **1** (Figure 1) were prepared by reacting 1,2-bis-(dichlorophosphino)ethane with Ar<sup>F</sup>MgBr or Ar<sup>F</sup>Li in Et<sub>2</sub>O or THF.<sup>12</sup> Before investigating the reductive elimination, we studied the electronic effects induced by **1** with fluorinated phenyl groups on the central metal, because electronic effects are affected by steric influences for some bidentate ligands.<sup>13</sup> In particular, it is known that fluorine atoms at the 2,6-positions of aryl groups on phosphorus significantly increase the steric effects of phosphine ligands on the metal complex.<sup>14,15</sup> The electronic effects of diphosphine ligands on the central metal were evaluated by comparing the highest infrared CO stretching frequencies ( $\nu_{\text{CO}}$ ) for *cis*-Mo[diphosphine](CO)<sub>4</sub> complexes (**2**, Table 1),<sup>15,16</sup> which were synthesized from Mo(norbornadiene)(CO)<sub>4</sub>. As expected, the  $\sigma$ -donating ability of **1** tended to decrease with increasing number of fluorine atoms on the diphosphine aromatic rings. Interestingly, the  $\sigma$ -donating ability of diphosphines bearing 2,6-fluorinated aryl groups was slightly lower than those bearing the same number of fluorine atoms at different positions. This can be explained by the inductive effect of the Ar<sup>F</sup> group on the diphosphine. The  $\nu_{\text{CO}}$  values of **2** including nonaromatic diphosphine-ligated complexes were highly correlated with Taft's  $\sigma^*$  values (Figure 2,  $r^2 > 0.99$ ),<sup>17,18</sup> which closely correlate with the basicity of the corresponding phosphines,<sup>19</sup> suggesting that the  $\nu_{\text{CO}}$  values are mainly induced by not steric but electronic effects of diphosphine. In other

(13) Küendig, E. P.; Dupre, C.; Bourdin, B.; Cunningham, A., Jr.; Pons, D. *Helv. Chim. Acta* **1994**, *772*, 421.

(14) Cone angle of PAR<sub>3</sub> bearing 2,6-fluorinated aryl (C<sub>6</sub>F<sub>5</sub> = 184° or 172°; 2,6-F<sub>2</sub>C<sub>6</sub>H<sub>3</sub> = 176° or 171°) is greatly larger than that bearing 2,6-norfluorinated aryl (3,4,5-F<sub>3</sub>C<sub>6</sub>H<sub>2</sub> = 4-FC<sub>6</sub>H<sub>4</sub> = Ph = 145°) (ref 12b).

(15) Cone angle of dfppe (151°) vs dppe (125°): Ernst, M. F.; Roddick, D. M. *Inorg. Chem.* **1989**, *28*, 1624.

(16) Hoge, B.; Panne, P. *Chem.—Eur. J.* **2006**, *12*, 9025.

(17) The  $\nu_{\text{CO}}$  values of monophosphine ligands are highly correlated with its Taft's  $\sigma^*$  values: Bigorgne, M. J. *Inorg. Nucl. Chem.* **1964**, *26*, 107.

(18) Korenaga, T.; Kadowaki, K.; Ema, T.; Sakai, T. *J. Org. Chem.* **2004**, *69*, 7340.

(19) Babji, C.; Poë, A. J. *J. Phys. Org. Chem.* **2004**, *17*, 162.

## Scheme 1. Reductive Elimination from 3

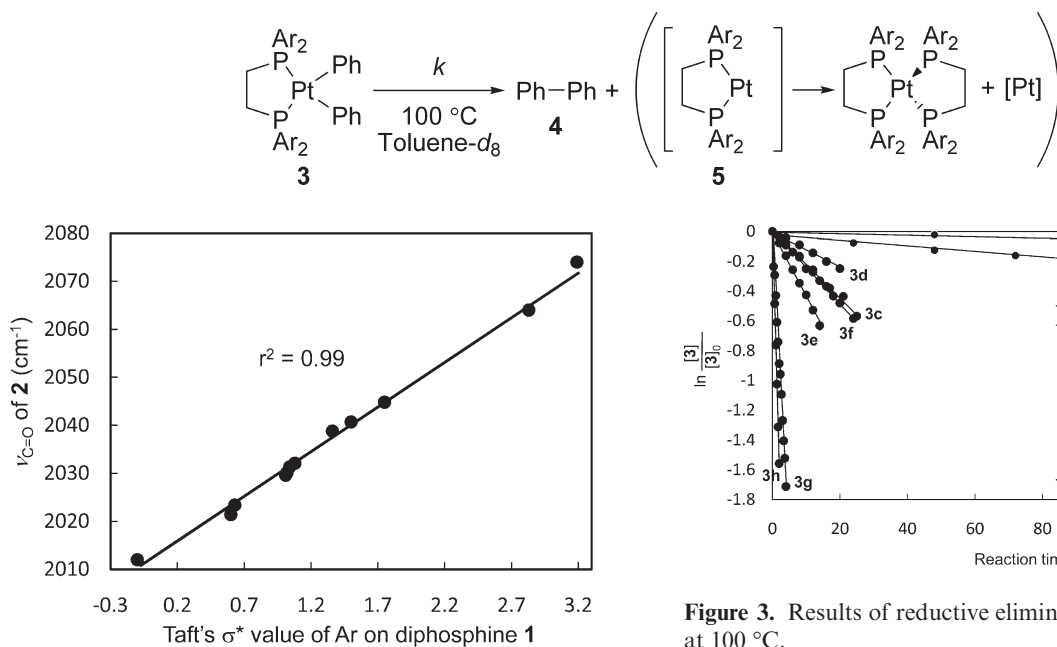


Figure 2. Correlation between Taft's  $\sigma^*$  of Ar in **1** and  $\nu_{\text{C}=\text{O}}$  of **2**.

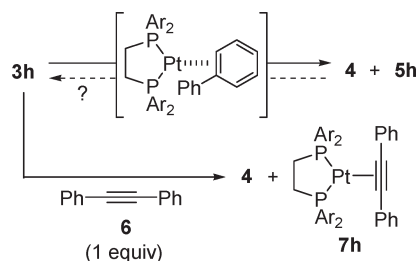
words, the electronic nature of the diphosphine ligands is reflected directly in the molybdenum d orbitals.

**Synthesis of *cis*-[Pt(Ph)<sub>2</sub>(diphosphine)] (**3**).** *cis*-[Pt(Ph)<sub>2</sub>(diphosphine)] complexes (**3**) were prepared using (COD)-PtCl<sub>2</sub> as a starting material. The diphosphines (**1**) reacted with (COD)PtCl<sub>2</sub> to give the corresponding *cis*-[Pt(Cl)<sub>2</sub>(**1**)] complexes, which were treated with PhMgBr to produce platinum complexes **3a–h**. Complex **3i**, which bears heptafluorotolyl groups, could not be isolated because the reductive elimination proceeded at ambient temperature. A similar result had been observed by Roddick et al. in the case of *cis*-[Pt(Ph)<sub>2</sub>(dfepc)] [dfepc = (C<sub>2</sub>F<sub>5</sub>)<sub>2</sub>PCH<sub>2</sub>CH<sub>2</sub>P(C<sub>2</sub>F<sub>5</sub>)<sub>2</sub>], whose complex was more unstable thermally than **3i**.<sup>10</sup> <sup>31</sup>P NMR spectra for all synthesized complexes **3** showed a single resonance peak with <sup>195</sup>Pt satellites, whose coupling constants <sup>1</sup>J<sub>Pt–P</sub> were within ca. 1500 to 1700 Hz. These results indicate that all complexes **3** were *cis*-isomers<sup>20</sup> with C<sub>2</sub> symmetry.

**Experimental Study of Reductive Elimination of Biphenyl from **3**.** The reductive elimination of biphenyl from complex **3** is shown in Scheme 1. The recrystallized complexes **3** and degassed *d*<sub>8</sub>-toluene were placed in an NMR tube under an argon atmosphere. The sealed NMR tube was immersed in an oil bath, which was maintained constant at 100 ± 0.1 °C, and the reaction was monitored by <sup>1</sup>H NMR.

The reaction rate of the reductive elimination ( $k$ ) was measured by comparing the integral values of phenyl protons in complex **3** and biphenyl (**4**). The kinetic data are summarized in Figure 3. The decomposition of complex **3** was adequately described by a pseudo-first-order rate law ( $r^2 > 0.99$ ). This is consistent with results obtained for **3h** by Roddick et al., who reported that the reductive elimination gave Pt(dfppe)<sub>2</sub> through a coordinatively unsaturated 14e Pt(dfppe) complex (**5h**) in an aromatic solvent.<sup>10</sup> However, the existence of a reverse reaction between highly reactive **5** and **4** could not be completely denied.

Figure 3. Results of reductive elimination from **3** in *d*<sub>8</sub>-toluene at 100 °C.

Scheme 2. Capture of Reactive Species **5h** by the Addition of **6**

Therefore, the reductive elimination of **3h** was performed in the presence of diphenylacetylene (**6**), which traps the 14e Pt complex to give a stable platinum alkyne complex (**7h**) (Scheme 2).<sup>21</sup> <sup>1</sup>H NMR analysis for an equimolar mixture of **3h** and **6** in *d*<sub>8</sub>-toluene clearly showed four-proton signals for **3h** ( $\delta = 6.79$  ppm) and **6** ( $\delta = 7.46$  ppm) initially. After heating for several minutes at 100 °C, equal amounts of **4** ( $\delta = 7.40$  ppm) and complex **7h** ( $\delta = 7.74$  ppm)<sup>22</sup> were generated, while the amounts of **3h** and **6** decreased. This suggests that **6** captures **5h** immediately without significant side reaction. The reaction of **3h** in the presence of **6** also followed a pseudo-first-order rate law, and the rate constant was evaluated to be  $2.25 \times 10^{-4} \text{ s}^{-1}$ , similar to the reaction without **6** ( $k = 2.23 \times 10^{-4} \text{ s}^{-1}$ ) (Figure 3). Furthermore, the rate constant of **3h** in the presence of 1.0 equiv of additional **4** also showed a similar value ( $k = 2.30 \times 10^{-4} \text{ s}^{-1}$ ). These results suggest that the reverse reaction between **5h** and **4** does not occur; in other words, the reaction rate of **3h** shows the rate of reductive elimination itself.

The reductive elimination of dfppe complex **3h** was found to be the fastest, with a rate constant that is 1240 times greater than that for dppe complex **3a** (Figure 3). This 3 order

(20) <sup>1</sup>J<sub>PtP</sub> of *cis*-[PtPh<sub>2</sub>(PPh<sub>3</sub>)<sub>2</sub>] = 1762 Hz, *cis*-[PtPh<sub>2</sub>(PMe<sub>2</sub>Ph)<sub>2</sub>] = 1754 Hz, *trans*-[PtPh<sub>2</sub>(PMe<sub>2</sub>Ph)<sub>2</sub>] = 2916 Hz in CD<sub>2</sub>Cl<sub>2</sub>; Nilsson, P.; Plamper, F.; Wendt, O. F. *Organometallics* **2003**, *22*, 5235.

(21) (a) Ozawa, F.; Hikida, T.; Hayashi, T. *J. Am. Chem. Soc.* **1994**, *116*, 2844. (b) Ozawa, F.; Hikida, T.; Hasebe, K.; Mori, T. *Organometallics* **1998**, *17*, 1018. (c) Hasebe, K.; Kamite, J.; Mori, T.; Katayama, H.; Ozawa, F. *Organometallics* **2000**, *19*, 2022.

(22) Complex **7h** was confirmed by alternative synthesis according to the procedure of the synthesis of [Pt(dppe)(6)]: Müller, C.; Iverson, C. N.; Lachicotte, R. J.; Jones, W. D. *J. Am. Chem. Soc.* **2001**, *123*, 9718.

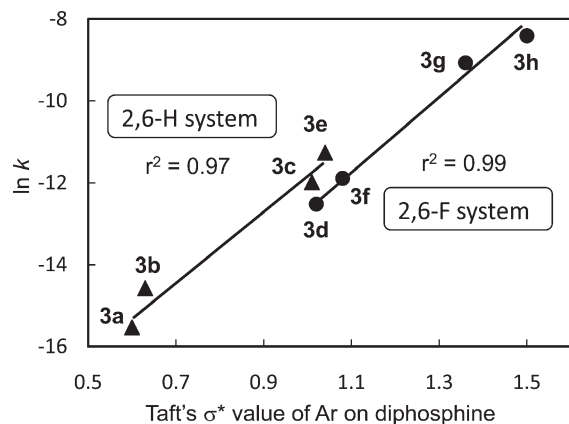


**Figure 4.** Correlation between Taft's  $\sigma^*$  of Ar in **1** and  $\ln k$  of **3**.

of magnitude difference is rare for ligand electronic effects, though large bite angles in bidentate ligands are known to increase rate constants by more than a factor of  $10^3$ , as mentioned above. The reaction rate constants increased with increasing number of fluorine atoms in the diphosphine ligands, indicating that the reaction rates depend on the electron-withdrawing strength of the diphosphine ligands. However, when the phosphines contained the same number of fluorine atoms, reaction rates observed for complexes with 2,6-fluorinated phenyl-bound diphosphines such as **3d** and **3f** were smaller than for complexes that did not contain 2,6-fluorinated phenyl-bound diphosphines such as **3c** and **3e**. This result does not agree with the trends shown by the  $\nu_{\text{CO}}$  values for Mo(diphosphine)(CO)<sub>4</sub> and Taft's  $\sigma^*$  values (Table 1). Strong correlations were actually obtained between  $\ln k$  and Taft's  $\sigma^*$  values for diphosphine aryl groups (Figure 4) when the diphosphines were split into two systems ( $r^2 = 0.97$  and  $0.99$ ). The 2,6-H system consisted of complexes **3a**, **3b**, **3c**, and **3e**, which did not contain fluorine atoms at the 2- and 6-positions of the diphosphine aryl groups. The 2,6-F system consisted of complexes **3d**, **3f**, **3g**, and **3h**, with diphosphines containing 2,6-fluorinated phenyl groups. This result indicates that differences in diphosphine steric and electronic effects on platinum exist between 2,6-H and 2,6-F system complexes, despite an acceleration of the reaction induced by an increase in fluorine atom numbers in the diphosphines. The correlation between  $\ln k$  and the  $^1J_{\text{Pt-P}}$  coupling constant of complex **3** also showed variations in the ligand effects on reaction rates (Figure 5). The correlations were determined by dividing the diphosphines into 2,6-H and 2,6-F systems, whose correlation coefficients were over 0.99. The strong correlations between  $\ln k$  and  $^1J_{\text{Pt-P}}$  suggested that the electronic nature of the diphosphines played a dominant role in reductive elimination rates for each system. The kinetic parameters of the reductive eliminations were estimated within 90–110 °C (80–105 °C for **3h**) to obtain further information (Table 2). The calculated parameters gave significant information regarding differences between 2,6-H and 2,6-F system trends. Higher  $\Delta H_{\text{obs}}^\ddagger$  values were obtained for the 2,6-H system compared to the 2,6-F system, consistent with the trend obtained from Taft's  $\sigma^*$  values for diphosphine aryl groups and with the  $\nu_{\text{CO}}$  values of a molybdenum complex (Table 1). However, unlike the trend of electron-donating ability of diphosphines, the  $\Delta H_{\text{obs}}^\ddagger$  value was greater for **3e**, which contains 3,4,5-trifluorophenyl, than for **3d**, which contains 2,6-difluorophenyl. This result suggests the existence of conformational differences between 2,6-H and 2,6-F systems. Furthermore, a small discrepancy in  $\Delta S_{\text{obs}}^\ddagger$  values between 2,6-H (ca. 11 cal

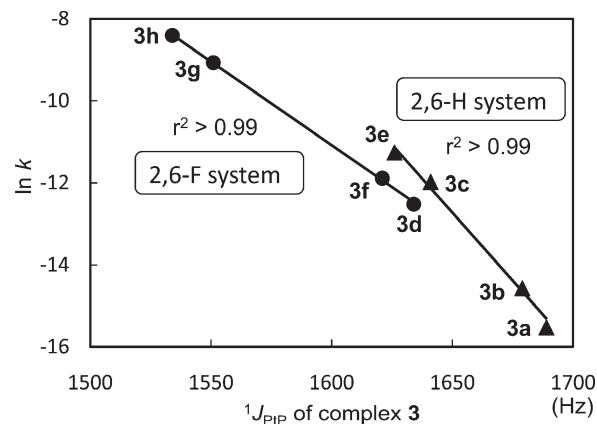


**Figure 5.** Correlation between  $^1J_{\text{Pt-P}}$  of **3** and  $\ln k$  of **3**.

**Table 2.** Activation Parameters of Reductive Elimination from **3**<sup>a</sup>

complex [2,6-]	$\Delta H_{\text{obs}}^\ddagger$ (kcal mol <sup>-1</sup> )	$\Delta S_{\text{obs}}^\ddagger$ (cal mol <sup>-1</sup> K <sup>-1</sup> )	$\Delta G_{\text{obs}}^\ddagger$ <sup>100</sup> (kcal mol <sup>-1</sup> )
<b>3a</b> [H]	37.8 ± 1.4 <sup>b</sup>	11.5 ± 1.6 <sup>b</sup>	33.5
<b>3b</b> [H]	37.2 ± 1.2 <sup>b</sup>	11.8 ± 1.3 <sup>b</sup>	32.8
<b>3c</b> [H]	35.0 ± 0.2 <sup>b</sup>	11.0 ± 0.6 <sup>b</sup>	30.9
<b>3d</b> [F]	31.7 ± 1.1 <sup>b</sup>	1.1 ± 0.9 <sup>b</sup>	31.3
<b>3e</b> [H]	34.7 ± 0.2 <sup>c</sup>	11.6 ± 0.6 <sup>c</sup>	30.3
<b>3f</b> [F]	30.9 ± 0.7 <sup>c</sup>	0.1 ± 0.5 <sup>c</sup>	30.8
<b>3g</b> [F]	29.1 ± 0.1 <sup>c</sup>	1.0 ± 0.5 <sup>c</sup>	28.7
<b>3h</b> [F]	28.7 ± 0.2 <sup>d</sup>	1.4 ± 0.5 <sup>d</sup>	28.2

<sup>a</sup> Activation enthalpies ( $\Delta H_{\text{obs}}^\ddagger$ ) and entropies ( $\Delta S_{\text{obs}}^\ddagger$ ) were determined by Arrhenius plots for the thermolysis of complex **3** within. <sup>b</sup> 100–110 °C. <sup>c</sup> 90–110 °C. <sup>d</sup> 80–105 °C.

mol<sup>-1</sup> K<sup>-1</sup>) and 2,6-F systems (ca. 1 cal mol<sup>-1</sup> K<sup>-1</sup>) may suggest similar differences in both systems. The experimental values were interpreted using DFT calculations. In particular, we focused on clarifying (1) the nature of diphosphine electronic effects and (2) the effect of diphosphine 2,6-fluorine atoms on reductive elimination.

**Computational Analysis of Reductive Elimination. A. Conformational Discussion of Complexes **3** and TS-3.** We performed a computational analysis of the reductive elimination of **3** (details are described in the Experimental Section). All optimized structures are shown in the Supporting Information. In the cases of complexes **3a**, **3b**, **3c**, and **3e** in the 2,6-H system, we found three conformers (Figure 6, A–C), depending on the conformation of the diphosphine aryl groups. Among them, conformer B was the most stable conformation by ca. 1 kcal mol<sup>-1</sup> as compared to the other conformers. Therefore, we decided that the starting materials from the 2,6-H system would be conformer B for reductive elimination.<sup>23</sup> On the other hand, the optimization of complexes **3d**, **3f**, **3g**, and **3h** from the 2,6-F system produces only conformer A. The structures were validated by comparison with the crystal structure of **3d** (Supporting Information, Figure S25).<sup>23</sup>

The reductive elimination of **3** proceeds through either direct or dissociative reaction paths.<sup>1b</sup> The optimizations of transition states **3a–3h-TS** from a direct path and **3a–3h-TS'** from a dissociative path gave the single conformers, respectively. The activation energies ( $\Delta E_a$ ) were calculated by subtracting the energy of the starting material (**3**) from the energy of the transition state (**3-TS** or **3-TS'**), which corresponded to a direct path or dissociative path, respectively (Table 3). In all cases the

(23) A detailed discussion is described in the Supporting Information.

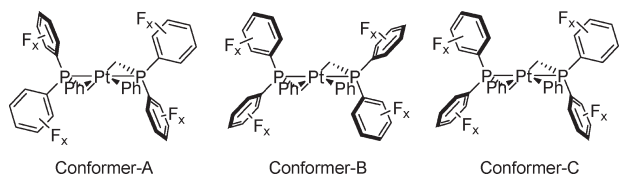


Figure 6. Possible conformations of complexes **3**.

Table 3. Calculated Activation Energies from **3** to **3-TS**

ligand	$\Delta E_a$ (kcal mol <sup>-1</sup> ) <sup>a,b</sup>		
	<b>3</b> to <b>3-TS</b>	<b>3</b> to <b>3-TS'</b>	
2,6-H system	<b>1a</b>	30.35	36.37
	<b>1b</b>	30.09	36.01
	<b>1c</b>	28.01	33.08
	<b>1e</b>	27.66	32.44
2,6-F system	<b>1d</b>	27.18	32.24
	<b>1f</b>	26.61	31.82
	<b>1g</b>	25.50	29.95
	<b>1h</b>	25.06	29.79

<sup>a</sup>All structures were optimized at the B3LYP/6-31G\* (LANL2DZ for Pt) level. The energies were calculated at the same level with ZPE correction. <sup>b</sup> $\Delta E_a$  = (energy of **3-TS**) – (energy of **3**).

dissociative path required a larger  $\Delta E_a$  by ca. 5–6 kcal mol<sup>-1</sup> as compared with those of the direct path. Therefore, we concluded that the reductive elimination of **3** proceeded through the direct path.<sup>24</sup> The values of  $\Delta E_a$  in **3** to **3-TS** were highly correlated with experimentally observed  $\Delta H^\ddagger_{\text{obs}}$  values in Table 2 (Figure 7), indicating that our calculated models are reliable for evaluating reductive elimination.

**B. Steric Effects: Bond Lengths and Angles of Complexes **3** and **3-TS**.** The calculated bond lengths and angles are summarized in Table S1 in the Supporting Information for complexes **3** and **3-TS**. The bite angles ( $\beta$ , Figure 8) of 2,6-H type complexes **3** were slightly wider (ca. 0.1–0.3°) than for 2,6-F type complexes, in concert with the C<sup>1</sup>–Pt–C<sup>2</sup> angles being narrower, and the C<sup>1</sup>...C<sup>2</sup> distances were shortened with larger bite angles. However, small differences in  $\beta$ , C<sup>1</sup>–Pt–C<sup>2</sup>, and C<sup>1</sup>...C<sup>2</sup> do not significantly impact the reductive elimination. In transition states **3-TS**, C<sup>1</sup>–Pt–C<sup>2</sup> was broadened within ca. 1.3° and C<sup>1</sup>...C<sup>2</sup> was lengthened within ca. 0.04 Å with increasing number of fluorine atoms. This suggests that the transition states in the cases of electron-poor diphosphines lie slightly toward the starting material because of electron-withdrawing effects. Although this trend is identical to a

(24) The bite angle of dppe in the geometry where dissociation from palladium(II) is not easy: Moiseev, D. V.; Malysheva, Y. B.; Shavyrin, A. S.; Kurskii, Y. A.; Gushchin, A. V. *J. Organomet. Chem.* **2005**, 690, 3652.

(25) This trend has been sometimes observed in the crystal structure bearing a fluoroaromatic phosphine: (a) Wursche, R.; Debaerdemaeker, T.; Klinga, M.; Rieger, B. *Eur. J. Inorg. Chem.* **2000**, 9, 2063. (b) Atherton, M. J.; Coleman, K. S.; Fawcett, J.; Holloway, J. H.; Hope, E. G.; Karacar, A.; Peck, L. A.; Saunders, G. C. *J. Chem. Soc., Dalton Trans.* **1995**, 4029.

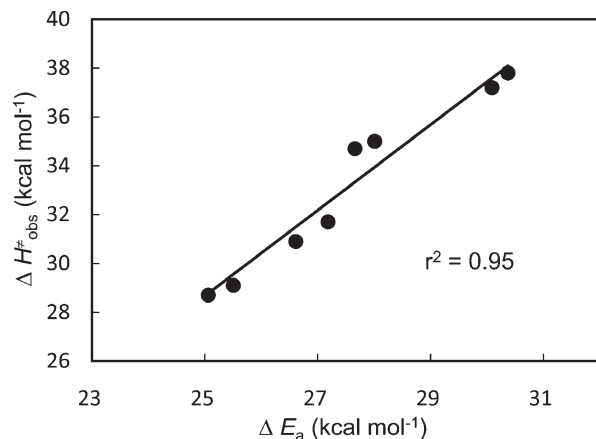


Figure 7. Correlation between calculated  $\Delta E_a$  and experimental  $\Delta H^\ddagger_{\text{obs}}$ .

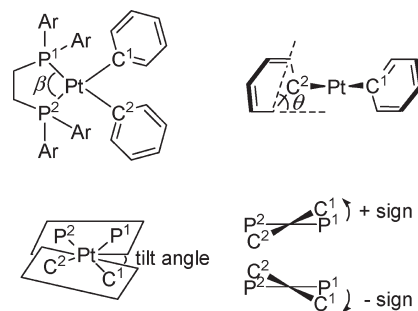
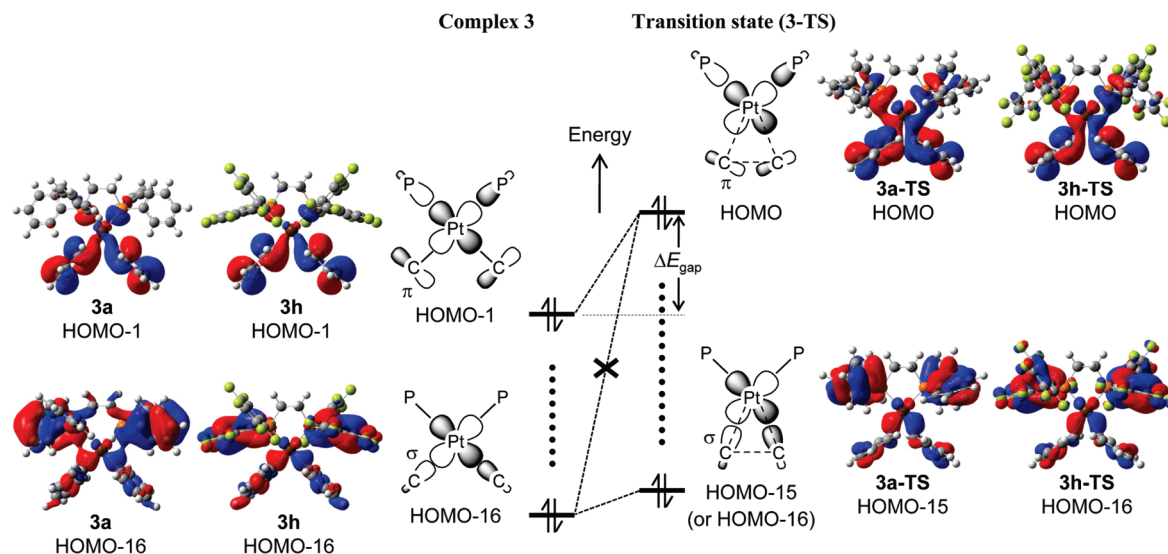


Figure 8. Definition of angles for **3** and **3-TS**.

previous report,<sup>11c</sup> the structural changes were very small. The P<sup>1</sup>–Pt bond lengths shortened with an increasing number of fluorine atoms in **3** and **3-TS**.<sup>25</sup> However, no meaningful differences were observed for C<sup>1</sup>–Pt bond lengths, suggesting that the *trans* influence of the diphosphine on the reactive phenyl groups made no difference. The values of  $\theta$  (Figure 8) were smaller for 2,6-F-type complexes **3** than for the 2,6-H system and tended to decrease with increasing number of fluorine atoms. A greater difference between 2,6-F and 2,6-H systems was attributed to the twist of the diphosphine aryl groups in conformers A and B. A similar trend was found in **3-TS**, but the difference was smaller compared to **3**. The values of  $\theta$  in 2,6-H (90.5–90.8°) and in 2,6-F systems (88.8–88.3°) were close to the ideal angle (90°), indicating that the conformations facilitate the overlap of the reactive phenyl sp<sup>2</sup> orbitals at the C<sup>1</sup>-position regardless of the diphosphine. A larger difference in the tilt angle (Figure 8) was found in the 2,6-H system in **3-TS** compared to **3**.<sup>26</sup> Relatively large changes in tilt angles from **3** to **3-TS** in the 2,6-H system would result in significantly different activation parameters compared to the 2,6-F system.

Overall, the electronic effect of diphosphines on the structures of complexes **3** and **3-TS** was found to be small. Although steric effects of diphosphines also had little effect on  $\beta$  and C<sup>1</sup>–Pt–C<sup>2</sup> bond angles and P<sup>1</sup>–Pt and C<sup>1</sup>–Pt bond lengths, they were shown to influence the conformation of the diphosphine aryl groups (Figure 6, Conformer-A vs. B) and the twist of the reactive phenyl rings (see Supporting Information, Figures S19–S21). These results would impact the differences in  $\Delta H^\ddagger$  and  $\Delta S^\ddagger$  between 2,6-H and 2,6-F systems and can be used to compare

(26) Ananikov, V. P.; Musaev, D. G.; Morokuma, K. *Organometallics* **2005**, 24, 715.



**Figure 9.** Schematic correlation diagram between **3** and **3-TS**.

differences in reactivity between both systems. However, they do not provide explanations for diphosphine electronic effects on the acceleration of reductive elimination.

**C. Electronic Effect of Diphosphine.** To obtain information regarding diphosphine electronic effects on reductive elimination, we first focused on the platinum electron density in complex **3**, because the electron density of the central metal is generally supposed to influence reductive elimination.<sup>1</sup> Platinum atomic charges in complex **3** were calculated to give Mulliken and NPA charges.<sup>27</sup> However, no good correlation was observed between  $\Delta H^\ddagger_{\text{obs}}$  and the platinum atomic charge in complex **3** (Supporting Information, Table S2, Figure S26).

In the reductive elimination of *cis*-d<sup>8</sup>L<sub>2</sub>MR<sub>2</sub> (M = Ni, Pd, Pt) through a direct path, two electrons are transferred into the d orbital of M, and then two M–R bond cleavages and R–R bond formations occur to give d<sup>10</sup>L<sub>2</sub>M and R<sub>2</sub>. Therefore, the d orbital of the transition-state HOMO plays a significant role in the reductive elimination at this stage. The d<sub>x<sup>2</sup>-y<sup>2</sup> orbitals of platinum in the transition state were located in the HOMO of **3-TS** (Figure 9).<sup>11c,28</sup> The same d orbitals were found in HOMO–1 and HOMO–16 of complex **3** (Figure 9), in which the orbital symmetry was the same as for the HOMO of **3-TS**. In an early study of the reductive elimination from [PdMe<sub>2</sub>(PH<sub>3</sub>)<sub>2</sub>] using EHMO calculations, the bonding b<sub>2</sub> orbital of [PdMe<sub>2</sub>(PH<sub>3</sub>)<sub>2</sub>], which had two Pd–C σ-bonding orbitals, was shown to be highly correlated to the activation energy of the reductive elimination.<sup>11a</sup> This result suggested that the b<sub>2</sub> orbital, which was the lowest d orbital, was linked to the transition-state HOMO. The orbital of complex **3** corresponding to its b<sub>2</sub> orbital was HOMO–16, which had two Pt–C σ-bonding orbitals (Figure 9). However, HOMO–16 of **3** did not appear to be linked to the HOMO of **3-TS**, because the HOMO of **3-TS** had π orbitals at the reactive phenyl instead of Pt–C σ-bonding orbitals. Therefore, the HOMO of **3-TS** was connected to the HOMO–1 of **3**, which also had π orbitals at the reactive phenyl. On the other hand, the HOMO–16 of **3** was linked to</sub>

**Table 4.** Orbital Energies of HOMO–1 in **3** and HOMO in **3-TS**

	ligand	orbital energy (eV) <sup>a</sup>		$\Delta E_{\text{gap}}$ (eV) <sup>b</sup>
		<b>3</b> (HOMO–1)	<b>3-TS</b> (HOMO)	
2,6-H system	<b>1a</b>	–5.290	–3.639	1.650
	<b>1b</b>	–5.503	–3.866	1.637
	<b>1c</b>	–5.647	–4.069	1.577
	<b>1e</b>	–5.833	–4.268	1.566
2,6-F system	<b>1d</b>	–5.139	–3.588	1.552
	<b>1f</b>	–5.336	–3.814	1.522
	<b>1g</b>	–5.507	–4.038	1.469
	<b>1h</b>	–5.682	–4.236	1.446

<sup>a</sup> Orbital energies were calculated at the B3LYP/6-31G\* (LANL2DZ for Pt) level. <sup>b</sup>  $\Delta E_{\text{gap}} = (\text{energy of HOMO in } \mathbf{3-TS}) - (\text{energy of HOMO-1 in } \mathbf{3})$ .

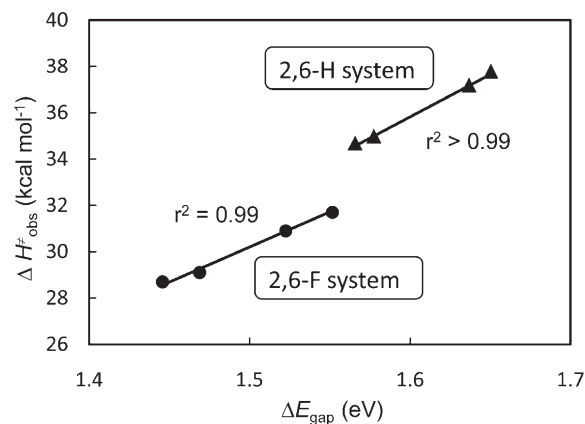


**Figure 10.** Correlation between  $\Delta E_{\text{gap}}$  and  $\Delta H^\ddagger_{\text{obs}}$ .

the HOMO–16 or HOMO–15 of **3-TS**, which had Pt–C σ-bonding orbitals (Figure 9). The higher energy of HOMO–1 of **3** relative to HOMO–16 of **3** narrows the energy difference with the HOMO of **3-TS**. This is consistent with the fact that the reductive elimination of two phenyl groups bearing π orbitals is significantly faster than for two methyl groups bearing only σ orbitals.<sup>11c,26</sup> The energy gap between the HOMO–1 of **3** and the HOMO of **3-TS** ( $\Delta E_{\text{gap}}$ ) showed a linear correlation with  $\Delta H^\ddagger$  for the 2,6-H and 2,6-F systems (Table 4, Figure 10). This result suggests that these d orbitals play a significant role in the reductive elimination and that electron-poor diphosphines

(27) ESP charges (CHelpG) on platinum showed negative values. See also the following report: Zimmermann, T.; Zeizinger, M.; Burda, J. V. *J. Inorg. Biochem.* **2005**, *99*, 2184.

(28) Perez-Rodriguez, M.; Braga, A. A. C.; Garcia-Melchor, M.; Perez-Temprano, M. H.; Casares, J. A.; Ujaque, G.; de Lera, A. R.; Alvarez, R.; Maseras, F.; Espinet, P. *J. Am. Chem. Soc.* **2009**, *131*, 3650.

**Table 5. Energies of 3, 3-TS, and Fragment Structures<sup>a</sup>**

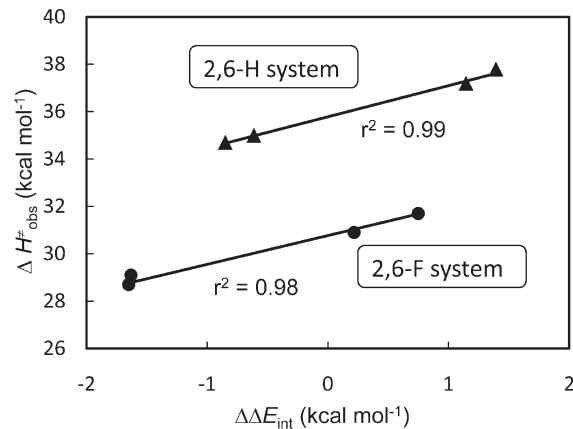
	ligand	$\Delta E_{\text{int}}^{\ddagger}$ (kcal mol <sup>-1</sup> ) <sup>b</sup>	$\Delta E_{\text{int}}^{\ddagger}$ (kcal mol <sup>-1</sup> ) <sup>c</sup>	$\Delta\Delta E_{\text{int}}^{\ddagger}$ (kcal mol <sup>-1</sup> ) <sup>d</sup>
2,6-H system	<b>1a</b>	-51.04	-49.65	1.39
	<b>1b</b>	-49.07	-47.93	1.14
	<b>1c</b>	-43.86	-44.47	-0.61
	<b>1e</b>	-42.23	-43.07	-0.84
2,6-F system	<b>1d</b>	-41.52	-40.77	0.75
	<b>1f</b>	-39.27	-39.05	0.22
	<b>1g</b>	-35.15	-36.78	-1.63
	<b>1h</b>	-33.48	-35.13	-1.65

<sup>a</sup> Energies were calculated at the B3LYP/6-31G\* (LANL2DZ for Pt) level without ZPE correction. <sup>b</sup>  $\Delta E_{\text{int}}^{\ddagger}$  = (energy of **3**) - (energy of [Pt-Ph<sub>2</sub>] + [L<sub>2</sub>]). <sup>c</sup>  $\Delta E_{\text{int}}^{\ddagger}$  = (energy of **3-TS**) - (energy of [Pt-Ph<sub>2</sub>]<sup>‡</sup> + [L<sub>2</sub>]<sup>‡</sup>). <sup>d</sup>  $\Delta\Delta E_{\text{int}}^{\ddagger}$  =  $\Delta E_{\text{int}}^{\ddagger}$  -  $\Delta E_{\text{int}}$ .

decrease  $\Delta E_{\text{gap}}$  to lower the reaction energy barrier. Although  $\Delta E_{\text{gap}}$  values decreased with increasing number of fluorine atoms in each system, the values were not proportional to the overall electron-withdrawing ability of **1**.

To obtain information on the electronic effects of diphosphine, the energies of fragment structures were calculated by the DFT method. The structures of **3** and **3-TS** were divided into diphosphine fragments ([L<sub>2</sub>] or [L<sub>2</sub>]<sup>‡</sup>) and PtPh<sub>2</sub> fragments ([Pt-Ph<sub>2</sub>] or [Pt-Ph<sub>2</sub>]<sup>‡</sup>) with the same geometry as the original optimized structures.<sup>11c</sup> The calculated energies are summarized in Table 5. The energy difference ( $\Delta E_{\text{int}}$ ) between **3** and [L<sub>2</sub>] + [Pt-Ph<sub>2</sub>] was considered as the interaction energy between the diphosphine and platinum complex, and  $\Delta E_{\text{int}}^{\ddagger}$  represents the interaction energy in the transition states in the same way. Both  $\Delta E_{\text{int}}$  and  $\Delta E_{\text{int}}^{\ddagger}$  values were negative and tended to increase with increasing number of fluorine atoms. This indicates that the diphosphine significantly stabilizes the nonligated 12e platinum-diphenyl complex and that stronger  $\sigma$ -donating diphosphines stabilize this 12e complex to a greater extent. The results show that the diphosphines stabilized platinum through  $\sigma$ -donation rather than  $\pi$ -back-donation.<sup>29</sup> The  $\Delta\Delta E_{\text{int}}$  values were calculated from the difference between  $\Delta E_{\text{int}}^{\ddagger}$  and  $\Delta E_{\text{int}}$ . Negative  $\Delta\Delta E_{\text{int}}$  values thus suggest that the stabilization by diphosphine is greater in **3-TS** than in **3**. The calculated  $\Delta\Delta E_{\text{int}}$  values were highly correlated to  $\Delta H_{\text{obs}}^{\ddagger}$  in each system (Figure 11), indicating that the electron-poor diphosphine stabilizes transition state **3-TS** rather than reactant **3** to lower the reaction energy barrier.<sup>11c</sup> However, the existence of the two correlations showed that the stabilization did not originate from diphosphine electronic effects only.

Next, we focused on the orbital energies of the fragment structures (Table 6). The HOMO-2 of [Pt-Ph<sub>2</sub>] fragments displayed the same orbital symmetry as the HOMO-1 in complex **3**. Similarly, the HOMO in [Pt-Ph<sub>2</sub>]<sup>‡</sup> fragments corresponded to the HOMO in **TS-3**. The energy differences between the corresponding orbitals,  $\Delta E_{\text{MO}}$  = (energy of HOMO-1 in **3**) - (energy of HOMO-2 in [Pt-Ph<sub>2</sub>]) and  $\Delta E_{\text{MO}}^{\ddagger}$  = (energy of HOMO in **3-TS**) - (energy of HOMO in [Pt-Ph<sub>2</sub>]<sup>‡</sup>), were considered as the stabilization energy of the platinum d orbital upon binding with diphosphine. All  $\Delta E_{\text{MO}}$  and  $\Delta E_{\text{MO}}^{\ddagger}$  were positive, indicating that the platinum d orbitals were destabilized upon binding with diphosphines. This destabilization results from the P-Pt  $\sigma^*$ -antibonding character (see Supporting Information, Figure S27), which disfavors the strong  $\sigma$ -donating character of diphosphines.<sup>11c</sup> The decrease in  $\Delta E_{\text{MO}}$  and  $\Delta E_{\text{MO}}^{\ddagger}$  values with increasing number of fluorine atoms suggests that electron-poor diphosphines tend to ease the destabilization. The values of

**Figure 11.** Correlation between  $\Delta\Delta E_{\text{int}}$  and  $\Delta H_{\text{obs}}^{\ddagger}$ .

$\Delta\Delta E_{\text{MO}}$ , whose positive values mean that the destabilization of the platinum d orbital upon binding to diphosphine is larger in **3-TS** than in **3**, identified the nature of diphosphine electronic effects in the reductive elimination. A good correlation was obtained between  $\Delta\Delta E_{\text{MO}}$  and  $\Delta H_{\text{obs}}^{\ddagger}$  regardless of the presence of 2,6-difluorine atoms (Figure 12), suggesting that highly electron-poor diphosphines may reduce the destabilization in **3-TS** relative to the cases of less electron-poor diphosphines to decrease the activation enthalpy.

## Conclusion

Through the study of the reductive elimination of biphenyl from **3**, we obtained the following conclusions.

(1) The reductive elimination of biphenyl from *cis*-[Pt(Ph)<sub>2</sub>(diphosphine)] was found to be highly accelerated by the electronic effects of electron-poor diphosphines. The fastest reaction, which was observed for **3h**, is over 1000 times faster than the slowest reaction.

(2) The nature of the diphosphine ligand effects on reductive elimination was separated into steric 2,6-fluorine effects and genuine electronic effects. The existence of 2,6-fluorine or 2,6-hydrogen atoms in the aryl rings on phosphorus strongly influenced the conformations of starting complex **3** and transition state **3-TS** to give two correlations between *k* (or  $\Delta H_{\text{obs}}^{\ddagger}$ ) and several parameters.

(3) Strong correlations showed that diphosphine electronic effects were the main factor in the reductive elimination rates, although the results were also influenced by steric effects. The correlation between  $\Delta H_{\text{obs}}^{\ddagger}$  and platinum electron density in **3** was not satisfactory, but the d orbital energy gap between HOMO-1 in **3** and the HOMO in **3-TS** was highly correlated with  $\Delta H_{\text{obs}}^{\ddagger}$ . The electron-poor diphosphines decrease the energy gap to decrease the reaction energy barrier. Reasons for this decrease in energy gap are that (a) the stabilization of **3-TS** by electron-poor diphosphines exceeds that of **3** and (b) the destabilization of the platinum d orbital upon binding to diphosphines in **3-TS** is reduced by electron-poor diphosphines, which is the nature of diphosphine electronic effects on reductive elimination from **3**. These results show the electronic effects of diphosphines on the reductive elimination of biphenyl from platinum complexes.

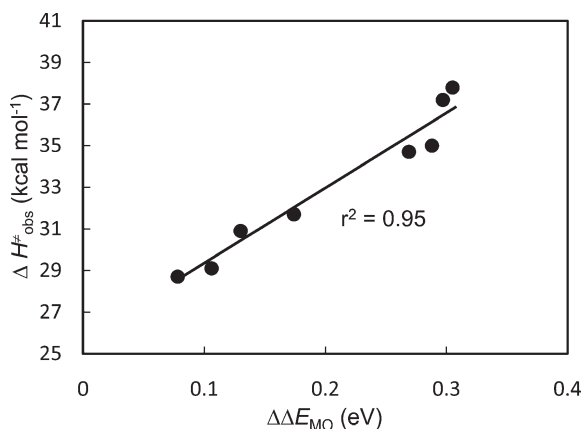
Although only one aspect of ligand effects could be shown, the conclusions are not always applicable to other reductive elimination systems. For example, differences in the central metals will cause changes in the d orbital energy order, and

(29) (a) Yamanaka, M.; Shiga, A. *J. Theor. Comput. Chem.* **2005**, *4*, 345. (b) Yamanaka, M.; Mikami, K. *Organometallics* **2005**, *24*, 4579.

**Table 6. Orbital Energies of 3, 3-TS, and Fragment Structures**

ligand	orbital energy (eV) <sup>a</sup>			orbital energy (eV) <sup>a</sup>			$\Delta\Delta E_{MO}$ (eV) <sup>d</sup>	
	3, HOMO-1	[Pt-Ph <sub>2</sub> ], HOMO-2	$\Delta E_{MO}$ (eV) <sup>b</sup>	3-TS, HOMO	[Pt-Ph <sub>2</sub> ] <sup>‡</sup> , HOMO	$\Delta E_{MO}^{\ddagger}$ (eV) <sup>c</sup>		
2,6-H system	<b>1a</b>	-5.290	-6.496	1.206	-3.639	-5.150	1.511	0.305
	<b>1b</b>	-5.503	-6.499	0.996	-3.866	-5.159	1.293	0.297
	<b>1c</b>	-5.647	-6.463	0.816	-4.069	-5.173	1.104	0.288
2,6-F system	<b>1e</b>	-5.833	-6.475	0.642	-4.268	-5.179	0.911	0.269
	<b>1d</b>	-5.139	-6.540	1.401	-3.588	-5.163	1.575	0.174
	<b>1f</b>	-5.336	-6.566	1.230	-3.814	-5.174	1.360	0.130
	<b>1g</b>	-5.507	-6.571	1.064	-4.038	-5.208	1.170	0.106
	<b>1h</b>	-5.682	-6.585	0.903	-4.236	-5.217	0.981	0.078

<sup>a</sup>Orbital energies were calculated at the B3LYP/6-31G\* (LANL2DZ for Pt) level. <sup>b</sup> $\Delta E_{MO}$  = (energy of HOMO-1 in **3**) - (energy of HOMO-2 in [Pt-Ph<sub>2</sub>]). <sup>c</sup> $\Delta E_{MO}^{\ddagger}$  = (energy of HOMO in **3-TS**) - (energy of HOMO in [Pt-Ph<sub>2</sub>]<sup>‡</sup>). <sup>d</sup> $\Delta\Delta E_{MO}$  =  $\Delta E_{MO}^{\ddagger}$  -  $\Delta E_{MO}$ .

**Figure 12.** Correlation between  $\Delta\Delta E_{MO}$  and  $\Delta H^{\ddagger}_{obs}$ .

the reaction following the dissociative path will result in different orbital states in the transition state compared to the reaction following the direct path. These cases might lead to different results and conclusions. However, the correlation method between experimental and theoretical values that we performed in this study will play an important role in clarifying other mechanisms for the reductive elimination reaction.

## Experimental Section

**General Experimental Methods.** All reactions were carried out under an argon atmosphere with dry solvents under anhydrous conditions, unless otherwise noted. Dehydrated benzene, dichloromethane, hexane, tetrahydrofuran (THF), diethyl ether, and toluene were purchased from Kanto Chemical Co., Inc. and then were stored in Schlenk tubes under an argon atmosphere. 1,2-Bis[bis(pentafluorophenyl)phosphino]ethane (DFPPE) was purchased from Sigma-Aldrich. 1,2-Bis(diphenylphosphino)ethane (DPPE)

was purchased from Kanto Chemical Co., Inc. Other reagents were purchased at the highest commercial quality and used without further purification, unless otherwise noted. Preparative column chromatography was carried out by using silica gel (Fuji Silysia BW-127 ZH, 100–270 mesh). <sup>1</sup>H NMR and <sup>13</sup>C NMR spectra were measured at 300 or 500 MHz and 75 or 125 MHz or 150 MHz, respectively, and chemical shifts are given relative to tetramethylsilane (TMS). <sup>19</sup>F NMR spectra were measured at 282 MHz, and chemical shifts are given relative to CCl<sub>3</sub>F using C<sub>6</sub>F<sub>6</sub> as a secondary reference (-162.9 ppm). <sup>31</sup>P NMR spectra were measured at 121 MHz, and chemical shifts are given relative to 85% H<sub>3</sub>PO<sub>4</sub> as an external standard. Thermolysis samples were heated in an oil bath (Mini-heater MH-5E, Riko).

**[1,2-Bis{diphenylphosphino}ethane]tetracarbonylmolybdenum [2a].**<sup>30</sup> Dppe (51.5 mg, 129 μmol) and [Mo(CO)<sub>4</sub>(nbd)] (46.2 mg, 154 μmol) were dissolved in 4 mL of dichloroethane, and then the solution was stirred for 3 h at 60 °C under argon atmosphere. The filtered solution was concentrated under reduced pressure. The desired product was purified by recrystallization from CH<sub>2</sub>Cl<sub>2</sub>-hexane. The white crystalline product was obtained in a yield of 74% (58.3 mg). Mp: 190–191 °C (dec). <sup>1</sup>H NMR (acetone-*d*<sub>6</sub>, 300 MHz): δ 2.71–2.87 (m, 4H), 7.38–7.47 (m, 12H), 7.67–7.74 (m, 8H). <sup>31</sup>P NMR (acetone-*d*<sub>6</sub>, 121 MHz): δ 59.5 (s). IR (CH<sub>2</sub>Cl<sub>2</sub>): 2021.4, 1912, 1884, 1099, 895, and 587 cm<sup>-1</sup>.

**[1,2-Bis{bis(4-fluorophenyl)phosphino}ethane]tetracarbonylmolybdenum [2b].** Complex **2b** was prepared similarly to the synthesis of **2a** from [Mo(CO)<sub>4</sub>(nbd)] (58.9 mg, 196 μmol) and 1,2-bis[bis(4-fluorophenyl)phosphino]ethane (80.3 mg, 171 μmol). The white crystalline product was obtained in a yield of 65% (75.2 mg). Mp: 178–179 °C (dec). <sup>1</sup>H NMR (acetone-*d*<sub>6</sub>, 300 MHz): δ 2.75–2.89 (m, 4H), 7.22–7.29 (m, 8H), 7.71–7.80 (m, 8H). <sup>19</sup>F NMR (acetone-*d*<sub>6</sub>, 282 MHz): δ -107.8 (s, 4F). <sup>31</sup>P NMR (acetone-*d*<sub>6</sub>, 121 MHz): δ 59.1 (s). IR (CH<sub>2</sub>Cl<sub>2</sub>): 2023.4, 1912, 1889, 1592, 1496, 1235, 1162, 1096, and 828 cm<sup>-1</sup>. Anal. Calcd for C<sub>30</sub>H<sub>20</sub>F<sub>4</sub>MoO<sub>4</sub>P<sub>2</sub>: C, 53.12; H, 2.97. Found: C, 53.03; H, 3.14.

(30) Grim, O. G.; Briggs, W. L.; Barth, R. C.; Tolman, C. A.; Jesson, J. P. *Inorg. Chem.* **1974**, *13*, 1095.

**[1,2-Bis{bis(3,5-difluorophenyl)phosphino}ethane]tetracarbonylmolybdenum [2c].** Complex **2c** was prepared similarly to the synthesis of **2a** from  $[\text{Mo}(\text{CO})_4(\text{nbd})]$  (45.9 mg, 153  $\mu\text{mol}$ ) and 1,2-bis[bis(3,5-difluorophenyl)phosphino]ethane (73.3 mg, 135  $\mu\text{mol}$ ). The white crystalline product was obtained in a yield of 60% (61.0 mg). Mp: 175–176 °C (decompose).  $^1\text{H}$  NMR (acetone- $d_6$ , 300 MHz):  $\delta$  3.04–3.13 (m, 4H), 7.13–7.24 (m, 4H), 7.34–7.44 (m, 8H).  $^{19}\text{F}$  NMR (acetone- $d_6$ , 282 MHz):  $\delta$  –104.6 (s, 8F).  $^{31}\text{P}$  NMR (acetone- $d_6$ , 121 MHz):  $\delta$  67.4 (s). IR ( $\text{CH}_2\text{Cl}_2$ ): 2029.6, 1921, 1608, 1590, 1421, 1288, 1125, 988, and 860  $\text{cm}^{-1}$ . Anal. Calcd for  $\text{C}_{30}\text{H}_{16}\text{F}_8\text{MoO}_4\text{P}_2$ : C, 48.02; H, 2.15. Found: C, 48.20; H, 2.07.

**[1,2-Bis{bis(2,6-difluorophenyl)phosphino}ethane]tetracarbonylmolybdenum [2d].**<sup>12b</sup> Complex **2d** was prepared similarly to the synthesis of **2a** from  $[\text{Mo}(\text{CO})_4(\text{nbd})]$  (58.1 mg, 194  $\mu\text{mol}$ ) and 1,2-bis[bis(2,6-difluorophenyl)phosphino]ethane (92.3 mg, 170  $\mu\text{mol}$ ). The white crystalline product was obtained in a yield of 70% (89.7 mg). Mp: 195–196 °C (dec).  $^1\text{H}$  NMR (300 MHz, acetone- $d_6$ ):  $\delta$  3.04–3.11 (m, 4H), 7.04–7.11 (m, 8H), 7.53–7.63 (m, 4H).  $^{19}\text{F}$  NMR (acetone- $d_6$ , 282 MHz):  $\delta$  –97.1 (s, 8F).  $^{31}\text{P}$  NMR (acetone- $d_6$ , 121 MHz):  $\delta$  32.2 (s). IR ( $\text{CH}_2\text{Cl}_2$ ): 2030.1, 1939, 1916, 1611, 1458, 1232, 1104, 987, and 791  $\text{cm}^{-1}$ .

**[1,2-Bis{bis(3,4,5-trifluorophenyl)phosphino}ethane]tetracarbonylmolybdenum [2e].** Complex **2e** was prepared similarly to the synthesis of **2a** from  $[\text{Mo}(\text{CO})_4(\text{nbd})]$  (59.0 mg, 197  $\mu\text{mol}$ ) and 1,2-bis[bis(3,4,5-trifluorophenyl)phosphino]ethane (106 mg, 173  $\mu\text{mol}$ ). The white crystalline product was obtained in a yield of 79% (112 mg). Mp: 221–222 °C (dec).  $^1\text{H}$  NMR (acetone- $d_6$ , 300 MHz):  $\delta$  3.05–3.15 (m, 4H), 7.52–7.60 (m, 8H).  $^{19}\text{F}$  NMR (acetone- $d_6$ , 282 MHz):  $\delta$  –154.8 to –154.6 (m, 4F), –129.8 to –129.7 (m, 8F).  $^{31}\text{P}$  NMR (acetone- $d_6$ , 121 MHz):  $\delta$  68.7 (s). IR ( $\text{CH}_2\text{Cl}_2$ ): 2031.3, 1941, 1922, 1616, 1522, 1419, 1320, 1081, 1051, and 897  $\text{cm}^{-1}$ . Anal. Calcd for  $\text{C}_{30}\text{H}_{12}\text{F}_{12}\text{MoO}_4\text{P}_2$ : C, 43.82; H, 1.47. Found: C, 43.61; H, 1.78.

**[1,2-Bis{bis(2,4,6-trifluorophenyl)phosphino}ethane]tetracarbonylmolybdenum [2f].** Complex **2f** was prepared similarly to the synthesis of **2a** from  $[\text{Mo}(\text{CO})_4(\text{nbd})]$  (52.5 mg, 175  $\mu\text{mol}$ ) and 1,2-bis[bis(2,4,6-trifluorophenyl)phosphino]ethane (80.9 mg, 132  $\mu\text{mol}$ ). The white crystalline product was obtained in a yield of 48% (52.4 mg). Mp: 181–182 °C (dec).  $^1\text{H}$  NMR (acetone- $d_6$ , 300 MHz):  $\delta$  3.03–3.10 (m, 4H), 7.03–7.10 (m, 8H).  $^{19}\text{F}$  NMR (acetone- $d_6$ , 282 MHz):  $\delta$  –100.9 to –100.8 (m, 4F), –94.0 to –93.9 (m, 8F).  $^{31}\text{P}$  NMR (acetone- $d_6$ , 121 MHz):  $\delta$  32.1 (s). IR ( $\text{CH}_2\text{Cl}_2$ ): 2032.1, 1942, 1920, 1630, 1605, 1586, 1429, 1171, 1126, 1084, 1006, 897, and 847  $\text{cm}^{-1}$ . Anal. Calcd for  $\text{C}_{30}\text{H}_{12}\text{F}_{12}\text{MoO}_4\text{P}_2$ : C, 43.82; H, 1.47. Found: C, 44.07; H, 1.63.

**[1,2-Bis{bis(2,3,5,6-tetrafluorophenyl)phosphino}ethane]tetracarbonylmolybdenum [2g].** Complex **2g** was prepared similarly to the synthesis of **2a** from  $[\text{Mo}(\text{CO})_4(\text{nbd})]$  (31.9 mg, 106  $\mu\text{mol}$ ) and 1,2-bis[bis(2,3,5,6-tetrafluorophenyl)phosphino]ethane (67.1 mg, 97.8  $\mu\text{mol}$ ). The white crystalline product was obtained in a yield of 45% (39.4 mg). Mp: 237–238 °C (dec).  $^1\text{H}$  NMR (acetone- $d_6$ , 300 MHz):  $\delta$  3.26–3.33 (m, 4H), 7.74–7.83 (m, 4H).  $^{19}\text{F}$  NMR (acetone- $d_6$ , 282 MHz):  $\delta$  –134.5 to –134.5 (m, 8F), –127.9 (m, 8F).  $^{31}\text{P}$  NMR (acetone- $d_6$ , 121 MHz):  $\delta$  40.3 (s). IR ( $\text{CH}_2\text{Cl}_2$ ): 2038.8, 1958, 1931, 1483, 1231, 1176, and 917  $\text{cm}^{-1}$ . Anal. Calcd for  $\text{C}_{30}\text{H}_8\text{F}_{16}\text{MoO}_4\text{P}_2$ : C, 40.29; H, 0.90. Found: C, 40.12; H, 0.57.

**[1,2-Bis{bis(pentafluorophenyl)phosphino}ethane]tetracarbonylmolybdenum [2h].**<sup>15</sup> Complex **2h** was prepared similarly to the synthesis of **2a** from  $[\text{Mo}(\text{CO})_4(\text{nbd})]$  (42.0 mg, 140  $\mu\text{mol}$ ) and dfppe (100 mg, 132  $\mu\text{mol}$ ). The white crystalline product was obtained in a yield of 24% (30.1 mg). Mp: 237–238 °C (dec).  $^1\text{H}$  NMR (acetone- $d_6$ , 300 MHz):  $\delta$  3.25–3.32 (m, 4H).  $^{19}\text{F}$  NMR (acetone- $d_6$ , 282 MHz):  $\delta$  –161.8 to –161.6 (m, 8F), –151.0 to –150.8 (m, 4F), –131.3 to –131.2 (m, 8F).  $^{31}\text{P}$  NMR (acetone- $d_6$ , 121 MHz):  $\delta$  35.8 (s). IR ( $\text{CH}_2\text{Cl}_2$ ): 2040.7, 1961, 1933, 1093, 981, and 894  $\text{cm}^{-1}$ .

**[1,2-Bis{bis(4-heptafluorotolyl)phosphino}ethane]tetracarbonylmolybdenum [2i].** Complex **2i** was prepared similarly to the

synthesis of **2a** from  $[\text{Mo}(\text{CO})_4(\text{nbd})]$  (34.4 mg, 115  $\mu\text{mol}$ ) and 1,2-bis[bis(4-heptafluorotolyl)phosphino]ethane (93.6 mg, 97.7  $\mu\text{mol}$ ). The yellow crystalline product was obtained in a yield of 46% (53.7 mg). Mp: 234–235 °C (dec).  $^1\text{H}$  NMR (acetone- $d_6$ , 300 MHz):  $\delta$  3.38–3.45 (m, 4H).  $^{19}\text{F}$  NMR (acetone- $d_6$ , 282 MHz):  $\delta$  –136.3 to –136.2 (m, 8F), –124.9 (m, 8F), –53.6 to –53.5 (m, 12F).  $^{31}\text{P}$  NMR (acetone- $d_6$ , 121 MHz):  $\delta$  43.6 (s). IR ( $\text{CH}_2\text{Cl}_2$ ): 2044.8, 1967, 1942, 1472, 1326, 1187, 1160, and 980  $\text{cm}^{-1}$ . Anal. Calcd for  $\text{C}_{34}\text{H}_4\text{F}_{28}\text{MoO}_4\text{P}_2$ : C, 35.02; H, 0.35. Found: C, 34.84; H, 0.63.

**[1,2-Bis{bis(4-fluorophenyl)phosphino}ethane]dichloroplatinum(II).** A solution of  $[\text{PtCl}_2(\text{cod})]$  (56.1 mg, 150  $\mu\text{mol}$ ) and **1b** (70.6 mg, 150  $\mu\text{mol}$ ) in toluene (3 mL) was stirred at reflux for 12 h under argon atmosphere. The reaction mixture was cooled to room temperature, and the insoluble white crystalline product was filtered and washed several times with diethyl ether in air. The white crystals were obtained in a yield of 93% (102 mg). Mp > 300 °C.  $^1\text{H}$  NMR (acetone- $d_6$ , 300 MHz):  $\delta$  2.63–2.76 (m, 4H), 7.31–7.35 (m, 8H), 7.99–8.05 (m, 8H).  $^{13}\text{C}$  NMR ( $\text{CD}_2\text{Cl}_2$ , 75 MHz):  $\delta$  27.6–29.3 (m), 115.9–116.3 (m), 121.5–122.8 (m), 135.3–135.9 (m), 163.1–166.5 (m).  $^{19}\text{F}$  NMR (acetone- $d_6$ , 282 MHz):  $\delta$  –105.2 (s, 4F).  $^{31}\text{P}$  NMR (acetone- $d_6$ , 121 MHz):  $\delta$  45.5 (s w/Pt-satellites,  $^1J_{\text{Pt-P}} = 3598$  Hz). IR (KBr): 1589, 1497, 1240, 1163, 1103, 829, and 530  $\text{cm}^{-1}$ . Anal. Calcd for  $\text{C}_{26}\text{H}_{20}\text{Cl}_2\text{F}_4\text{P}_2\text{Pt}$ : C, 42.41; H, 2.74. Found: C, 42.10; H, 2.74.

**[1,2-Bis{bis(3,5-difluorophenyl)phosphino}ethane]dichloroplatinum(II).** The title complex was prepared from  $[\text{PtCl}_2(\text{cod})]$  (56.1 mg, 150  $\mu\text{mol}$ ) and **1c** (81.4 mg, 150  $\mu\text{mol}$ ) in a similar manner to the synthesis of [1,2-bis{bis(4-fluorophenyl)phosphino}ethane]dichloroplatinum(II). The white crystalline product was obtained in a yield of 97% (118 mg). Mp > 300 °C.  $^1\text{H}$  NMR (acetone- $d_6$ , 300 MHz):  $\delta$  2.90–3.20 (m, 4H), 7.30–7.38 (m, 4H), 7.67–7.74 (m, 8H).  $^{19}\text{F}$  NMR (acetone- $d_6$ , 282 MHz):  $\delta$  –104.6 to –104.5 (m, 8F).  $^{31}\text{P}$  NMR (acetone- $d_6$ , 121 MHz):  $\delta$  49.0 (s w/Pt-satellites,  $^1J_{\text{Pt-P}} = 3594$  Hz). IR (KBr): 1653, 1589, 1425, 1294, 1124, 860, and 675  $\text{cm}^{-1}$ . Anal. Calcd for  $\text{C}_{26}\text{H}_{16}\text{Cl}_2\text{F}_8\text{P}_2\text{Pt}$ : C, 38.63; H, 2.00. Found: C, 38.33; H, 1.98.

**[1,2-Bis{bis(2,6-difluorophenyl)phosphino}ethane]dichloroplatinum(II).** The title complex was prepared from  $[\text{PtCl}_2(\text{cod})]$  (56.1 mg, 150  $\mu\text{mol}$ ) and **1d** (81.4 mg, 150  $\mu\text{mol}$ ) in a similar manner to the synthesis of [1,2-bis{bis(4-fluorophenyl)phosphino}ethane]dichloroplatinum(II). The white crystalline product was obtained in a yield of 84% (102 mg). Mp > 300 °C.  $^1\text{H}$  NMR (DMSO- $d_6$ , 300 MHz):  $\delta$  2.73–2.87 (m, 4H), 7.26–7.29 (m, 8H), 7.74–7.79 (m, 4H).  $^{19}\text{F}$  NMR (acetone- $d_6$ , 282 MHz):  $\delta$  –93.6 (s, 8F).  $^{31}\text{P}$  NMR (DMSO- $d_6$ , 121 MHz):  $\delta$  15.4 (s w/Pt-satellites,  $^1J_{\text{Pt-P}} = 3733$  Hz). IR (KBr): 1612, 1558, 1456, 1225, 1111, 986, and 791  $\text{cm}^{-1}$ . Anal. Calcd for  $\text{C}_{26}\text{H}_{16}\text{Cl}_2\text{F}_8\text{P}_2\text{Pt}$ : C, 38.63; H, 2.00. Found: C, 38.34; H, 2.20.

**[1,2-Bis{bis(3,4,5-trifluorophenyl)phosphino}ethane]dichloroplatinum(II).** The title complex was prepared from  $[\text{PtCl}_2(\text{cod})]$  (56.1 mg, 150  $\mu\text{mol}$ ) and **1e** (92.2 mg, 150  $\mu\text{mol}$ ) in a similar manner to the synthesis of [1,2-bis{bis(4-fluorophenyl)phosphino}ethane]dichloroplatinum(II). The white crystalline product was obtained in a yield of 94% (124 mg). Mp > 300 °C.  $^1\text{H}$  NMR (acetone- $d_6$ , 300 MHz):  $\delta$  2.99–3.10 (m, 4H), 7.87–7.93 (m, 8H).  $^{13}\text{C}$  NMR (acetone- $d_6$ , 125 MHz):  $\delta$  28.2–28.8 (m), 119.5–119.8 (m), 123.8–124.4 (m), 141.9–144.1 (m), 150.6–152.9 (m).  $^{19}\text{F}$  NMR (acetone- $d_6$ , 282 MHz):  $\delta$  –151.4 to –151.2 (m, 4F), –129.6 to –129.4 (m, 8F).  $^{31}\text{P}$  NMR (acetone- $d_6$ , 121 MHz):  $\delta$  48.2 (s w/Pt-satellites,  $^1J_{\text{Pt-P}} = 3606$  Hz). IR (KBr): 1618, 1526, 1421, 1325, 1090, 1051, and 625  $\text{cm}^{-1}$ . Anal. Calcd for  $\text{C}_{26}\text{H}_{12}\text{Cl}_2\text{F}_{12}\text{P}_2\text{Pt}$ : C, 35.47; H, 1.37. Found: C, 35.56; H, 1.08.

**[1,2-Bis{bis(2,4,6-trifluorophenyl)phosphino}ethane]dichloroplatinum(II).** The title complex was prepared from  $[\text{PtCl}_2(\text{cod})]$  (56.1 mg, 150  $\mu\text{mol}$ ) and **1f** (92.2 mg, 150  $\mu\text{mol}$ ) in a similar manner to the synthesis of [1,2-bis{bis(4-fluorophenyl)phosphino}ethane]dichloroplatinum(II). The white crystalline product was obtained in a yield of 94% (124 mg). Mp > 300 °C.

$^1\text{H}$  NMR (acetone- $d_6$ , 300 MHz):  $\delta$  2.90–3.09 (m, 4H), 7.12–7.19 (m, 8H).  $^{19}\text{F}$  NMR (acetone- $d_6$ , 282 MHz):  $\delta$  -97.7 to -97.6 (m, 4F), -90.4 (s, 8F).  $^{31}\text{P}$  NMR (acetone- $d_6$ , 121 MHz):  $\delta$  15.4 (s w/Pt-satellites,  $^1J_{\text{Pt-P}} = 3698$  Hz). IR (KBr): 1684, 1636, 1609, 1585, 1558, 1435, 1130, 1099, 1024, 1003, and 841  $\text{cm}^{-1}$ . Anal. Calcd for  $\text{C}_{26}\text{H}_{12}\text{Cl}_2\text{F}_{12}\text{P}_2\text{Pt}$ : C, 35.47; H, 1.37. Found: C, 35.47; H, 1.53.

**[1,2-Bis{bis(2,3,5,6-tetrafluorophenyl)phosphino}ethane]dichloroplatinum(II)**. The title complex was prepared from  $[\text{PtCl}_2(\text{cod})]$  (56.1 mg, 150  $\mu\text{mol}$ ) and **1g** (103 mg, 150  $\mu\text{mol}$ ) in a similar manner to the synthesis of [1,2-bis{bis(4-fluorophenyl)phosphino}ethane]dichloroplatinum(II). The white crystalline product was obtained in a yield of 95% (136 mg). Mp > 300 °C.  $^1\text{H}$  NMR (DMSO- $d_6$ , 300 MHz):  $\delta$  3.14–3.18 (m, 4H), 8.34–8.41 (m, 4H).  $^{19}\text{F}$  NMR (DMSO- $d_6$ , 282 MHz):  $\delta$  -133.6 to -133.4 (m, 8F), -124.2 to -124.1 (m, 8F).  $^{31}\text{P}$  NMR (DMSO- $d_6$ , 121 MHz):  $\delta$  21.9 (s w/Pt-satellites,  $^1J_{\text{Pt-P}} = 3681$  Hz). IR (KBr): 1522, 1477, 1240, and 1238  $\text{cm}^{-1}$ . Anal. Calcd for  $\text{C}_{26}\text{H}_8\text{Cl}_2\text{F}_{16}\text{P}_2\text{Pt}$ : C, 35.47; H, 1.37. Found: C, 32.79; H, 0.85.

**[1,2-Bis{bis(pentafluorophenyl)phosphino}ethane]dichloroplatinum(II)**.<sup>10</sup> The title complex was prepared from  $[\text{PtCl}_2(\text{cod})]$  (50.0 mg, 134  $\mu\text{mol}$ ) and DFPPE (**1h**) (101 mg, 133  $\mu\text{mol}$ ) in a similar manner to the synthesis of [1,2-bis{bis(4-fluorophenyl)phosphino}ethane]dichloroplatinum(II). The white crystalline product was obtained in a yield of 98% (133 mg). Mp > 300 °C.  $^1\text{H}$  NMR (acetone- $d_6$ , 300 MHz):  $\delta$  3.20–3.38 (m, 4H).  $^{13}\text{C}$  NMR (acetone- $d_6$ , 150 MHz):  $\delta$  30.5–31.4 (m), 101.3–102.0 (m), 138.0–139.9 (m), 144.6–146.5 (m), 147.4–149.3 (m).  $^{19}\text{F}$  NMR (acetone- $d_6$ , 282 MHz):  $\delta$  -157.2 to -157.1 (m, 8F), -142.6 to -142.4 (m, 4F), -123.5 to -123.4 (m, 8F).  $^{31}\text{P}$  NMR (acetone- $d_6$ , 121 MHz):  $\delta$  20.9 (s w/Pt-satellites,  $^1J_{\text{Pt-P}} = 3644$  Hz). IR (KBr): 1520, 1479, 1094, and 980  $\text{cm}^{-1}$ .

**[1,2-Bis{bis(4-heptafluorotolyl)phosphino}ethane]dichloroplatinum(II)**. The title complex was prepared from  $[\text{PtCl}_2(\text{cod})]$  (56.1 mg, 150  $\mu\text{mol}$ ) and **1i** (144 mg, 150  $\mu\text{mol}$ ) in a similar manner to the synthesis of [1,2-bis{bis(4-fluorophenyl)phosphino}ethane]dichloroplatinum(II). The white crystalline product was obtained in a yield of 96% (177 mg). Mp > 300 °C.  $^1\text{H}$  NMR (acetone- $d_6$ , 300 MHz):  $\delta$  3.39–3.58 (m, 4H).  $^{19}\text{F}$  NMR (acetone- $d_6$ , 282 MHz):  $\delta$  -135.7 to -135.8 (m, 8F), -121.1 to -121.2 (m, 8F), -54.0 to -53.8 (m, 12F).  $^{31}\text{P}$  NMR (acetone- $d_6$ , 121 MHz):  $\delta$  24.6 (s w/Pt-satellites,  $^1J_{\text{Pt-P}} = 3604$  Hz). IR (KBr): 1479, 1329, 1190, 1159, 982, 947, and 716  $\text{cm}^{-1}$ . Anal. Calcd for  $\text{C}_{30}\text{H}_4\text{Cl}_2\text{F}_{28}\text{P}_2\text{Pt}$ : C, 35.47; H, 1.37. Found: C, 35.56; H, 1.08.

**[1,2-Bis(diphenylphosphino)ethane]diphenylplatinum(II)** (**3a**).<sup>31</sup> To a slurry of  $[\text{PtCl}_2(\text{cod})]$  (206 mg, 550  $\mu\text{mol}$ ) in diethyl ether (29 mL) was added dropwise PhMgBr in diethyl ether (2.5 M, 490  $\mu\text{L}$ , 1.2 mmol), and the mixture was stirred for 13 h at room temperature under argon atmosphere. The reaction mixture was washed with saturated aqueous  $\text{NH}_4\text{Cl}$  in air. Then, the organic layer was dried over  $\text{MgSO}_4$ , filtered, and concentrated. The residue was recrystallized from  $\text{CH}_2\text{Cl}_2$ –pentane to give 177 mg of brown crystals (70%). Mp > 300 °C.  $^1\text{H}$  NMR ( $\text{CDCl}_3$ , 500 MHz):  $\delta$  2.51–2.55 (m, 8H), 5.15 (s w/Pt-satellites,  $^1J_{\text{Pt-H}} = 36.6$  Hz, 4H), 6.85–6.89 (m, 2H), 7.03–7.06 (m, 4H), 7.30 (m w/Pt-satellites,  $^3J_{\text{Pt-H}} = 69.3$  Hz, 4H).  $^{13}\text{C}$  NMR ( $\text{CDCl}_3$ , 125 MHz):  $\delta$  28.8, 104.3–104.7 (m), 122.8, 127.3–127.9 (m), 134.5–134.9 (m), 155.6.

$[\text{Pt}(\text{Ph})_2(\text{cod})]$  (62.0 mg, 136  $\mu\text{mol}$ ) and DPPE (**1a**) (54.0 mg, 136  $\mu\text{mol}$ ) in benzene (5.4 mL) were stirred for 1.5 h. The solvent was removed under reduced pressure, and the residue was recrystallized from  $\text{CH}_2\text{Cl}_2$ –hexane to give 71.4 mg of brown crystals (70%). Mp > 300 °C (dec).  $^1\text{H}$  NMR ( $\text{CDCl}_3$ , 300 MHz):  $\delta$  2.19–2.34 (m, 4H), 6.59–6.64 (m, 2H), 6.72–6.76 (m, 4H), 7.04–7.28 (m, 4H), 7.31–7.50 (m, 20H).  $^{13}\text{C}$  NMR ( $\text{CD}_2\text{Cl}_2$ , 75 MHz):  $\delta$  27.3–28.2 (m), 120.8–120.9 (m), 126.0–127.0 (m), 128.0–128.1 (m), 130.1, 130.6–131.5 (m), 132.8–133.1 (m),

136.2–136.7 (m), 160.4–162.0 (m).  $^{31}\text{P}$  NMR ( $\text{CDCl}_3$ , 121 MHz):  $\delta$  41.0 (s w/Pt-satellites,  $^1J_{\text{Pt-P}} = 1689$  Hz). IR (KBr): 3058, 1569, 1474, 1434, 1104, 1025, 876, 817, 748, 733, 727, 691, 680, and 528  $\text{cm}^{-1}$ .

**[1,2-Bis{bis(4-fluorophenyl)phosphino}ethane]diphenylplatinum(II)** (**3b**).<sup>32</sup> A slurry of [1,2-bis{bis(4-fluorophenyl)phosphino}ethane]dichloroplatinum(II) (102 mg, 139  $\mu\text{mol}$ ) in diethyl ether (7 mL) was cooled to -78 °C, and PhMgBr in diethyl ether (3 M, 280  $\mu\text{L}$ , 0.84 mmol) was added dropwise under argon atmosphere. The reaction mixture was stirred for 14 h at room temperature. The solvent was removed under reduced pressure, and the residue was dissolved in dichloromethane. The solution was washed with degassed water. The organic layer was dried over  $\text{MgSO}_4$ , and was filtered by glass wool. After concentration of the solution, hexane was added to the reaction mixture slowly. After standing at -20 °C for 16 h, the white crystals were obtained in a yield of 88% (101 mg). Mp > 250 °C (dec).  $^1\text{H}$  NMR ( $\text{CDCl}_3$ , 300 MHz):  $\delta$  2.14–2.27 (m, 4H), 6.63–6.67 (m, 2H), 6.76–6.80 (m, 4H), 7.00–7.26 (m, 12H), 7.37–7.45 (m, 8H).  $^{13}\text{C}$  NMR ( $\text{CDCl}_3$ , 125 MHz):  $\delta$  28.0–28.5 (m), 116.3–116.7 (m), 122.0, 127.4–127.9 (m), 128.0–128.4 (m), 136.5–136.6 (m), 137.5–137.8 (m), 161.5–162.5 (m), 164.0–166.0 (m).  $^{19}\text{F}$  NMR ( $\text{CDCl}_3$ , 282 MHz):  $\delta$  -110.2 to -110.3 (m, 4F).  $^{31}\text{P}$  NMR ( $\text{CDCl}_3$ , 121 MHz):  $\delta$  39.3 (s w/Pt-satellites,  $^1J_{\text{Pt-P}} = 1679$  Hz). IR (KBr): 1589, 1558, 1495, 1232, 1159, 1099, 827, 814, 729, 704, 527, and 517  $\text{cm}^{-1}$ .

**[1,2-Bis{bis(3,5-difluorophenyl)phosphino}ethane]diphenylplatinum(II)** (**3c**). The complex **3c** was prepared from [1,2-bis{bis(3,5-difluorophenyl)phosphino}ethane]dichloroplatinum(II) (93.0 mg, 115  $\mu\text{mol}$ ) and PhMgBr in diethyl ether (3 M, 240  $\mu\text{L}$ , 0.72 mmol) in a similar manner to the synthesis of **3b**. The white crystals were obtained in a yield of 76% (78 mg). Mp > 200 °C (dec).  $^1\text{H}$  NMR ( $\text{CDCl}_3$ , 300 MHz):  $\delta$  2.26–2.31 (m, 4H), 6.70–6.75 (m, 2H), 6.85–6.95 (m, 16H), 7.02–7.26 (m, 4H).  $^{13}\text{C}$  NMR (acetone- $d_6$ , 125 MHz):  $\delta$  27.6–28.1 (m), 107.1–107.5 (m), 116.9–117.2 (m), 122.7, 127.8–128.4 (m), 135.4–135.9 (m), 137.1–137.4 (m), 160.0–161.0 (m), 162.4–164.7 (m).  $^{19}\text{F}$  NMR ( $\text{CDCl}_3$ , 282 MHz):  $\delta$  -108.0 to -107.9 (m, 8F).  $^{31}\text{P}$  NMR ( $\text{CDCl}_3$ , 121 MHz):  $\delta$  42.0 (s w/Pt-satellites,  $^1J_{\text{Pt-P}} = 1641$  Hz). IR (KBr): 1609, 1587, 1420, 1292, 1123, 986, 854, 743, and 669  $\text{cm}^{-1}$ . Anal. Calcd for  $\text{C}_{38}\text{H}_{26}\text{F}_8\text{P}_2\text{Pt}$ : C, 51.19; H, 2.94. Found: C, 50.90; H, 3.13.

**[1,2-Bis{bis(2,6-difluorophenyl)phosphino}ethane]diphenylplatinum(II)** (**3d**). The complex **3d** was prepared from [1,2-bis{bis(2,6-difluorophenyl)phosphino}ethane]dichloroplatinum(II) (119 mg, 147  $\mu\text{mol}$ ) and PhMgBr in diethyl ether (3 M, 300  $\mu\text{L}$ , 0.90 mmol) in a similar manner to the synthesis of **3b**. The white crystals were obtained in a yield of 58% (76 mg). Mp > 300 °C (dec).  $^1\text{H}$  NMR ( $\text{CDCl}_3$ , 300 MHz):  $\delta$  2.71–2.81 (m, 4H), 6.48–6.53 (m, 2H), 6.60–6.64 (m, 4H), 6.76–6.80 (m, 8H), 6.90–7.20 (m, 4H), 7.29–7.35 (m, 4H).  $^{13}\text{C}$  NMR ( $\text{CD}_2\text{Cl}_2$ , 125 MHz):  $\delta$  28.3–29.0 (m), 106.4–107.9 (m), 111.4–111.7 (m),

(31) Appleton, T. G.; Bennett, M. A. *Inorg. Chem.* **1978**, *17*, 738.

(32) Clarke, M. L.; Heydt, M. *Organometallics* **2005**, *24*, 6475.

(33) Frisch, M. J.; Trucks, G. W.; Schlegel, H. B.; Scuseria, G. E.; Robb, M. A.; Cheeseman, J. R.; Montgomery, J. A., Jr.; Vreven, T.; Kudin, K. N.; Burant, J. C.; Millam, J. M.; Iyengar, S. S.; Tomasi, J.; Barone, V.; Mennucci, B.; Cossi, M.; Scalmani, G.; Rega, N.; Petersson, G. A.; Nakatsuji, H.; Hada, M.; Ehara, M.; Toyota, K.; Fukuda, R.; Hasegawa, J.; Ishida, M.; Nakajima, T.; Honda, Y.; Kitao, O.; Nakai, H.; Klene, M.; Li, X.; Knox, J. E.; Hratchian, H. P.; Cross, J. B.; Adamo, C.; Jaramillo, J.; Gomperts, R.; Stratmann, R. E.; Yazyev, O.; Austin, A. J.; Cammi, R.; Pomelli, C.; Ochterski, J. W.; Ayala, P. Y.; Morokuma, K.; Voth, G. A.; Salvador, P.; Dannenberg, J. J.; Zakrzewski, V. G.; Dapprich, S.; Daniels, A. D.; Strain, M. C.; Farkas, O.; Malick, D. K.; Rabuck, A. D.; Raghavachari, K.; Foresman, J. B.; Ortiz, J. V.; Cui, Q.; Baboul, A. G.; Clifford, S.; Cioslowski, J.; Stefanov, B. B.; Liu, G.; Liashenko, A.; Piskorz, P.; Komaromi, I.; Martin, R. L.; Fox, D. J.; Keith, T.; Al-Laham, M. A.; Peng, C. Y.; Nanayakkara, A.; Challacombe, M.; Gill, P. M. W.; Johnson, B.; Chen, W.; Wong, M. W.; Gonzalez, C.; Pople, J. A. *Gaussian 03*, Revision D.02 and E.01; Gaussian, Inc.: Wallingford, CT, 2004.

120.6, 125.6–126.6 (m), 132.6–132.9 (m), 134.7–135.2 (m), 158.7–160.5 (m), 161.2–164.7 (m).  $^{19}\text{F}$  NMR ( $\text{CDCl}_3$ , 282 MHz):  $\delta$  -99.6 (s, 8F).  $^{31}\text{P}$  NMR ( $\text{CDCl}_3$ , 121 MHz):  $\delta$  11.3 (s w/Pt-satellites,  $^1J_{\text{Pt-P}} = 1634$  Hz). IR (KBr): 1684, 1612, 1570, 1456, 1231, 986, and  $785\text{ cm}^{-1}$ . Anal. Calcd for  $\text{C}_{38}\text{H}_{26}\text{F}_8\text{P}_2\text{Pt}$ : C, 51.19; H, 2.94. Found: C, 50.89; H, 3.15.

Crystals of **3d** for X-ray analysis were obtained from  $\text{CH}_2\text{Cl}_2$ –hexane at room temperature. Crystal data and analysis results are given in the Supporting Information.

**[1,2-Bis{bis(3,4,5-trifluorophenyl)phosphino}ethane]diphenylplatinum(II) (3e)**. The complex **3e** was prepared from [1,2-bis{bis(3,4,5-trifluorophenyl)phosphino}ethane]dichloroplatinum(II) (132 mg, 150  $\mu\text{mol}$ ) and  $\text{PhMgBr}$  in diethyl ether (3 M, 300  $\mu\text{L}$ , 0.90 mmol) in a similar manner to the synthesis of **3b**. The white crystals were obtained in a yield of 67% (98 mg). Mp > 200 °C (dec).  $^1\text{H}$  NMR ( $\text{CDCl}_3$ , 300 MHz):  $\delta$  2.19–2.29 (m, 4H), 6.74–6.79 (m, 2H), 6.89–6.98 (m, 12H), 6.90–7.20 (m, 4H).  $^{13}\text{C}$  NMR (acetone- $d_6$ , 75 MHz):  $\delta$  27.2–28.0 (m), 118.6–119.3 (m), 122.8, 127.5–127.7 (m), 127.7–128.7 (m), 137.0–137.4 (m), 140.2–144.0 (m), 149.8–153.5 (m), 159.4–161.1 (m).  $^{19}\text{F}$  NMR ( $\text{CDCl}_3$ , 282 MHz):  $\delta$  -131.5 to -131.7 (m, 8F), -154.7 to -154.9 (m, 4F).  $^{31}\text{P}$  NMR ( $\text{CDCl}_3$ , 121 MHz):  $\delta$  41.2 (s w/Pt-satellites,  $^1J_{\text{Pt-P}} = 1626$  Hz). IR (KBr): 1684, 1558, 1522, 1418, 1323, and  $1049\text{ cm}^{-1}$ . Anal. Calcd for  $\text{C}_{38}\text{H}_{22}\text{F}_{12}\text{P}_2\text{Pt}$ : C, 47.37; H, 2.30. Found: C, 47.56; H, 2.68.

**[1,2-Bis{bis(2,4,6-trifluorophenyl)phosphino}ethane]diphenylplatinum(II) (3f)**. The complex **3f** was prepared from [1,2-bis{bis(2,4,6-trifluorophenyl)phosphino}ethane]dichloroplatinum(II) (124 mg, 141  $\mu\text{mol}$ ) and  $\text{PhMgBr}$  in diethyl ether (3 M, 280  $\mu\text{L}$ , 0.84 mmol) in a similar manner to the synthesis of **3b**. The white crystals were obtained in a yield of 76% (103 mg). Mp > 250 °C (dec).  $^1\text{H}$  NMR ( $\text{CDCl}_3$ , 300 MHz):  $\delta$  2.66–2.78 (m, 4H), 6.55–6.60 (m, 10H), 6.65–6.70 (m, 4H), 6.90–7.15 (m, 4H).  $^{13}\text{C}$  NMR ( $\text{CD}_2\text{Cl}_2$ , 75 MHz):  $\delta$  28.2–29.1 (m), 100.4–101.1 (m), 102.4–103.3 (m), 120.9–121.1 (m), 125.9–126.9 (m), 134.5–135.0 (m), 158.2–160.1 (m), 161.5–165.3 (m), 162.6–166.4 (m).  $^{19}\text{F}$  NMR ( $\text{CDCl}_3$ , 282 MHz):  $\delta$  -104.3 to -104.1 (m, 4F), -96.8 (s, 8F).  $^{31}\text{P}$  NMR ( $\text{CDCl}_3$ , 121 MHz):  $\delta$  11.0 (s w/Pt-satellites,  $^1J_{\text{Pt-P}} = 1621$  Hz). IR (KBr): 1632, 1605, 1585, 1429, 1171, 1128, 1092, 1024, 1003, 851, 841, 737, 729, 716, 702, and  $515\text{ cm}^{-1}$ . Anal. Calcd for  $\text{C}_{38}\text{H}_{22}\text{F}_{12}\text{P}_2\text{Pt}$ : C, 47.37; H, 2.30. Found: C, 47.10; H, 2.50.

**[1,2-Bis{bis(2,3,5,6-tetrafluorophenyl)phosphino}ethane]diphenylplatinum(II) (3g)**. The complex **3g** was prepared from [1,2-bis{bis(2,3,5,6-tetrafluorophenyl)phosphino}ethane]dichloroplatinum(II) (124 mg, 130  $\mu\text{mol}$ ) and  $\text{PhMgBr}$  in diethyl ether (3 M, 240  $\mu\text{L}$ , 0.72 mmol) in a similar manner to the synthesis of **3b**. The white crystals were obtained in a yield of 83% (112 mg). Mp > 200 °C (dec).  $^1\text{H}$  NMR (acetone- $d_6$ , 500 MHz):  $\delta$  3.12–3.19 (m, 4H), 6.49–6.52 (m, 2H), 6.64–6.68 (m, 4H), 6.90–7.17 (m, 4H), 7.67–7.74 (m, 4H).  $^{13}\text{C}$  NMR ( $\text{CD}_2\text{Cl}_2$ , 75 MHz):  $\delta$  28.2–28.9 (m), 109.0–109.6 (m), 121.7–121.8 (m), 126.3–127.3 (m), 133.9–134.4 (m), 143.9–147.9 (m), 156.7–158.6 (m), 162.7–164.7 (m).  $^{19}\text{F}$  NMR ( $\text{CDCl}_3$ , 282 MHz):  $\delta$  -137.9 to -138.0 (m, 8F), -130.4 (s, 8F).  $^{31}\text{P}$  NMR ( $\text{CDCl}_3$ , 121 MHz):  $\delta$  14.6 (s w/Pt-satellites,  $^1J_{\text{Pt-P}} = 1551$  Hz). IR (KBr,  $\text{cm}^{-1}$ ): 1653, 1558, 1481, 1373, 1234, 918, 735, and  $712\text{ cm}^{-1}$ . Anal. Calcd for  $\text{C}_{38}\text{H}_{18}\text{F}_{16}\text{P}_2\text{Pt}$ : C, 44.07; H, 1.75. Found: C, 44.37; H, 1.94.

**[1,2-Bis{bis(pentafluorophenyl)phosphino}ethane]diphenylplatinum(II) (3h)**.<sup>10</sup> The complex **3h** was prepared from [1,2-bis{bis(pentafluorophenyl)phosphino}ethane]dichloroplatinum(II) (77.0 mg, 75.2  $\mu\text{mol}$ ) and  $\text{PhMgBr}$  in diethyl ether (2 M, 140  $\mu\text{L}$ , 0.28 mmol) in a similar manner to the synthesis of **3b**. The white crystals were obtained in a yield of 64% (53 mg). Mp > 230 °C (dec).  $^1\text{H}$  NMR ( $\text{CDCl}_3$ , 500 MHz):  $\delta$  2.81–2.85 (m, 4H), 6.62–6.65 (m, 2H), 6.75–6.78 (m, 4H), 6.90–7.20 (m, 4H).  $^{13}\text{C}$  NMR ( $\text{CD}_2\text{Cl}_2$ , 75 MHz):  $\delta$  28.2–29.3 (m), 102.4–103.6 (m), 122.0–122.2 (m), 126.6–127.6 (m), 133.6–134.2 (m), 135.5–139.5 (m), 141.2–144.9 (m), 145.0–148.6 (m), 156.2–158.2 (m).  $^{19}\text{F}$  NMR ( $\text{CDCl}_3$ , 282 MHz):  $\delta$  -158.4 to

-158.3 (m, 8F), -146.4 to -146.2 (m, 4F), -125.7 to -125.6 (m, 8F).  $^{31}\text{P}$  NMR ( $\text{CDCl}_3$ , 121 MHz):  $\delta$  14.3 (s w/Pt-satellites,  $^1J_{\text{Pt-P}} = 1537$  Hz).

**[1,2-Bis{bis(pentafluorophenyl)phosphino}ethane]diiodoplatinum(II)**. To a solution of [(dfppe)PtCl<sub>2</sub>] (121 mg, 118  $\mu\text{mol}$ ) in  $\text{CH}_2\text{Cl}_2$  (15 mL) was added KI (102 mg, 614  $\mu\text{mol}$ ) under argon atmosphere. The reaction mixture was stirred overnight and was filtered through neutral alumina. The solvent was removed under reduced pressure. The residue was recrystallized from  $\text{CH}_2\text{Cl}_2$ –hexane to give 118 mg of light yellow crystals (83%). Mp > 300 °C (dec).  $^1\text{H}$  NMR (acetone- $d_6$ , 300 MHz):  $\delta$  2.95–3.12 (m, 4H).  $^{19}\text{F}$  NMR (acetone- $d_6$ , 282 MHz):  $\delta$  -157.3 to -157.2 (m, 8F), -142.6 to -142.5 (m, 4F), -123.6 to -123.4 (m, 8F).  $^{31}\text{P}$  NMR (acetone- $d_6$ , 121 MHz):  $\delta$  46.6 (s w/Pt-satellites,  $^1J_{\text{Pt-P}} = 3368$  Hz). IR (KBr): 1618, 1526, 1421, 1325, 1090, 1051, and  $625\text{ cm}^{-1}$ . Anal. Calcd for  $\text{C}_{26}\text{H}_4\text{I}_2\text{F}_{20}\text{P}_2\text{Pt}$ : C, 25.87; H, 0.33. Found: C, 25.79; H, 0.64.

**[1,2-Bis{bis(pentafluorophenyl)phosphino}ethane]diphenylacetyleneplatinum(II) (7h)**. To a solution of [(dfppe)PtI<sub>2</sub>] (118 mg, 97.8  $\mu\text{mol}$ ) in degassed 1,2-dichloroethane (25 mL) was added diphenylacetylene (17.5 mg, 98.2  $\mu\text{mol}$ ) under argon atmosphere. The reaction mixture was stirred at 80 °C for 1.5 h, and then the solvent was concentrated under reduced pressure. The resulting light yellow solid was dissolved in 25 mL of degassed ethanol,  $\text{NaBH}_4$  (8.6 mg, 0.23 mmol) in  $\text{H}_2\text{O}$  (4 mL) was added, and the mixture was then stirred for 3 h under argon atmosphere. The yellow precipitate was filtered quickly and was dried in vacuo. The solid was recrystallized from  $\text{CH}_2\text{Cl}_2$ –hexane to give 68.0 mg of light yellow crystals (61%).  $^1\text{H}$  NMR (acetone- $d_6$ , 300 MHz):  $\delta$  2.95–3.10 (m, 4H), 7.15–7.22 (m, 2H), 7.23–7.32 (m, 4H), 7.40–7.47 (m, 4H).  $^{13}\text{C}$  NMR (acetone- $d_6$ , 75 MHz):  $\delta$  31.3–32.2 (m), 109.0–110.0 (m), 127.8, 129.0, 130.3–130.9 (m), 134.2–134.5 (m), 136.8–140.9 (m), 141.8–145.9 (m), 146.0–149.5 (m).  $^{19}\text{F}$  NMR (toluene- $d_8$ , 282 MHz):  $\delta$  -160.7 to -160.5 (m, 8F), -149.0 to -148.8 (m, 4F), -132.3 to -132.2 (m, 8F).  $^{31}\text{P}$  NMR (toluene- $d_8$ , 121 MHz):  $\delta$  14.8 (s w/Pt-satellites,  $^1J_{\text{Pt-P}} = 3312$  Hz). IR (KBr): 1643, 1520, 1474, 1387, 1294, 1094, 976, 760, 692, and  $527\text{ cm}^{-1}$ . Anal. Calcd for  $\text{C}_{40}\text{H}_{14}\text{F}_{20}\text{P}_2\text{Pt}$ : C, 42.46; H, 1.25. Found: C, 42.09; H, 1.41.

**Theoretical Calculations.** Complexes **3** and the transition states, which were assumed to be **3-TS** from direct path or T-shaped structures (**3-TS'**, from dissociative path), were optimized by DFT calculations. All calculations were performed using the B3LYP functional as implemented in Gaussian 03.<sup>33</sup> The 6-31G(d) basis set was applied to all elements except Pt, which was described with the LANL2DZ effective core potential and the LANL2DZ basis set. Harmonic vibrational frequencies were computed for all stationary points in order to characterize them as local minima for **3** and saddle points for **3-TS** and **3-TS'**. The energies of optimized **3**, **3-TS**, and **3-TS'** were corrected using the zero-point energy. IRC calculations were performed to confirm biphenyl bond formation. Mulliken and NPA charges of optimized structure of **3** were calculated at the LANL2DZ level. The energies of the fragment structures of **3** and **3-TS** were calculated at the B3LYP/6-31G\* level for all atoms, except for Pt, which was computed using LANL2DZ.

**Acknowledgment.** This work was supported by JSPS KAKENHI (20550099). We thank Professor Fumiyouki Ozawa and Professor Kazuhiko Takai for helpful discussions, and Dr. Toshiyuki Oshiki for assistance with X-ray crystallography. We thank the SC-NMR Laboratory of Okayama University for  $^1\text{H}$ ,  $^{13}\text{C}$ ,  $^{19}\text{F}$ , and  $^{31}\text{P}$  NMR measurements.

**Supporting Information Available:** Experimental details of synthesis of ligands **1**, kinetic analyses, NMR data, crystallographic data, CIF file of **3d**, and computational details of **3**, **3-TS**, and **3-TS'**. This material is available free of charge via the Internet at <http://pubs.acs.org>.